

Agar-gelatin Maillard conjugates used for Pickering emulsion stabilization

Lipeng Du ^{a,b,c}, Yi Ru ^{a,b,c,d}, Huifen Weng ^{a,b,c,d}, Yonghui Zhang ^{a,b,c,d}, Jun Chen ^{a,b,c,d}, Anfeng Xiao ^{a,b,c,d,*}, Qiong Xiao ^{a,b,c,d,*}

^a College of Ocean Food and Biological Engineering, Jimei University, Xiamen 361021, PR China

^b National R&D Center for Red Alga Processing Technology, Xiamen 361021, PR China

^c Fujian Provincial Engineering Technology Research Center of Marine Functional Food, Xiamen 361021, PR China

^d Xiamen Key Laboratory of Marine Functional Food, Xiamen 361021, PR China

ARTICLE INFO

Keywords:

Agar
Gelatin
Maillard reaction
Pickering emulsions

ABSTRACT

A few protein- and polysaccharide-based particles have shown promising potential as stabilizers in multi-phase food systems. By incorporating polymer-based particles and modifying the wettability of colloidal systems, it is possible to create particle-stabilized emulsions with excellent stability. A Pickering emulsifier (AGMs) with better emulsifying properties was obtained by the Maillard reaction between acid-hydrolysed agar and gelatin. Laser confocal microscopy imaging revealed that AGMs particles can be used as solid emulsifiers to produce a typical O/W Pickering emulsion, with AGMs adsorbing onto the droplet surface to form a dense interfacial layer. Cryo-scanning electron microscopy analysis showed that AGMs self-assembled into a three-dimensional network structure, which prevented droplets aggregation through strong spatial site resistance, contributing to emulsion stabilization. These emulsions exhibited stability within a pH range of 1 to 11, NaCl concentrations not exceeding 300 mM, and at temperatures below 80 °C. The most stable emulsion oil-water ratio was 6:4 at a particle concentration of 0.75 % (w/v). AGMs-stabilized Pickering emulsion was utilized to create a semi-solid mayonnaise as a replacement for hydrogenated oil. Rheological analysis demonstrated that low-fat mayonnaise stabilized with AGMs exhibited similar rheological behavior to traditional mayonnaise, offering new avenues for the application of Pickering emulsions in the food industry.

1. Introduction

Recently, polysaccharides have attracted much attention as promising natural macromolecular materials due to their properties such as being widely available, renewable, environmentally biocompatible, and non-toxic. Agar is an anionic natural polysaccharide from red algae, consisting of long chains alternately linked to 1, 3-linked β-D-galactose and 1, 4-linked 3, 6-anhydru-α-L-galactose and with the sulfated functional groups (Roy et al., 2023). Because of its natural non-toxicity and unique gelling properties, agar is widely used in cosmetics, medicine, food, and other fields (Abdul Khalil et al., 2018). However, affected by the structure of its molecular chain and the type of functional groups, natural agar has shortcomings such as high brittleness, low transparency, and extreme hydrophilicity, which cannot satisfy the market's diversified needs for agar product performance (Chen et al., 2021; Zhang, Xiao, et al., 2023), so it is necessary to modify the structure of agar through physical, chemical, biological and other technical means to

change the nature of agar, thus giving agar new application properties. In order to change the structure of agar, many studies have used chemical modification methods, because it is more effective than physical methods and easier to operate than biotechnology. Using isopropyl alcohol as a solvent, caproic anhydride was introduced into the agar structure to obtain hexanoylated agar (HAG) and used as a Pickering stabilizer (Xiao, Chen, et al., 2022). Additionally, acylation and cross-linking with maleic anhydride (MA) and succinic anhydride (SA) resulted in a highly transparent agar without significantly decreasing its gel strength (Xiao, Ye, et al., 2022; Ye et al., 2022). Furthermore, grafting glutaric anhydride (GA) onto agar improved its freeze-thaw stability and swelling properties, and the hydrogel film prepared using GAG demonstrated specific absorption capacity for tetracycline hydrochloride in mildly acidic environments (Zhang, Ye, et al., 2023). However, such methods often require intricate processes or hazardous chemicals that restrict the application of the product in the food industry. Hence, a crucial approach is to modify agar using

* Corresponding authors at: College of Ocean Food and Biological Engineering, Jimei University, Xiamen 361021, PR China.

E-mail addresses: xxaaffeng@jmu.edu.cn (A. Xiao), xiaoqiong129@jmu.edu.cn (Q. Xiao).

environmentally friendly and safe techniques enabling its direct application in the food industry.

As a type of non-enzymatic browning reaction, Maillard conjugation is a green and safe modification strategy that takes place naturally with no additional chemical reagents during heat treatment (Aminikhah et al., 2023). From the chemical point of view, this reaction is generally based on covalent interactions among free amino residues of amino-containing compounds and carbonyl groups in reducing sugars. By linking protein and polysaccharide molecules through a simple Maillard reaction, it is expected to produce a coupling with the combined merits of both biopolymers. In recent years, most studies have found that Maillard couplings generally possess better emulsification properties (Kim et al., 2024; Wang et al., 2017; Wang et al., 2022). During the Maillard process, protein undergoes expansion and exposes more hydrophobic groups, this leads to the formation of amphiphilic conjugates that can firmly attach to the oil-water interface, creating a viscoelastic layer through the hydrophobic regions of the protein (Feng et al., 2022). Simultaneously, the polysaccharide regions of the conjugates can create a strong steric barrier, effectively preventing flocculation and coalescence (Kan et al., 2021). Therefore, protein-polysaccharide conjugates have garnered significant attention as novel emulsifiers. Soya isolate protein-dextran (SPI-D) couplings prepared using ultrasound and microwave-assisted Maillard were found to stabilize oil-in-water emulsions with good freeze-thaw stability (Zhang et al., 2017). Whey isolate protein and gum arabic conjugate (WPI-GA) produced by dry heating Maillard, stabilized β -carotene emulsions with improved environmental tolerance and higher bioaccessibility in vitro digestion simulations (Chen et al., 2022). The Maillard conjugates of κ -carrageenan (κ -Car) with milk protein isolate (MPI) prepared in a wet-heating system effectively improved the stability of oil-in-water emulsions, and the ice cream with the κ -Car/MPI conjugates exhibited greater resistance to melting due to its improved water-holding capacity (Seo & Oh, 2022; Seo & Yoo, 2021). We hypothesized that the presence of hydrochloric acid would cause the polysaccharide chain of agar to break, exposing its reducing ends and creating the possibility of a Maillard reaction with the free amino group in gelatin. This could lead to the production of agar-gelatin conjugates with improved emulsification properties through a Maillard reaction, making them useful as Pickering emulsifiers.

This study aimed to modify natural agar through the Maillard reaction to enhance its emulsifying properties. The agar-gelatin covalent was prepared by wet-heat Maillard reaction, and the emulsification activity and emulsion stability of agar (AG), gelatin (GE), a mixture of agar and gelatin (AGEs), and the conjugate of agar and gelatin (AGMs) were compared. The stability of Pickering emulsions stabilized by the AGEs particles were investigated under different preparation conditions such as particle concentration and oil phase, along with different environmental conditions such as pH, NaCl, and temperature. The stabilization mechanism of agar-gelatin-based Pickering emulsions was further revealed by microstructure observations of the emulsions. Finally, AGMs were applied to the preparation of low-fat mayonnaise to expand the application and value of agar in food processing. These results suggest that the Maillard reaction of agar and gelatin was a green and efficient method to improve the emulsification properties of agar and can be directly applied to foods.

2. Material and methods

2.1. Material

Agar with a molecular weight of 158,577 Da, gel strength of 1500 g/cm², sulfate content 0.53 %, gelling temperature of 37 °C, melting temperature of 94 °C, and moisture content ≤10 % was acquired from Greenfresh (Fujian) Food Stuff Co., Ltd. (Fujian, China). Gelatin with a gel strength of 200 g bloom (CAS: 9000-70-8) was purchased from Macklin Biochemical Co., Ltd. (Shanghai, China). Soybean oil, eggs were purchased from Pupu supermarket (Xiamen, China). Sodium hydroxide,

hydrochloric acid and sodium chloride were all analytical grade and bought from Sinopharm chemical reagent Co., Ltd. (Shanghai, China). All other chemicals were of analytical grade unless specified.

2.2. Preparation of acid-hydrolysis agars

To prepare acid-hydrolyzed agar powders, 20 g of agar powders were added to 200 mL of 1 mol/L hydrochloric acid solution. The mixture was stirred at ambient temperature using a magnetic stirrer (DLAB, MS-H-PRO+, Beijing, China) set at 500 rpm. After acid hydrolysis, the mixture was immediately filtered and washed with distilled water to remove excess hydrochloric acid. Then, 1 mol/L NaOH solution was added to adjust the pH to neutral, followed by washing with distilled water for 5–7 times. The resulting material was dried at 55 °C for 12 h and crushed to obtain acid-hydrolyzed agar powders. The duration of hydrolysis was 1 h and the amount of reducing sugar after hydrolysis was 6.84 % with hydrolysis before being 1.52 % according to the DNS method (Yu et al., 2020).

2.3. Preparation of agar-gelatin Maillard products

The agar-gelatin Maillard products were prepared using the wet-heating method, as described in previous studies (Huang et al., 2020; Zhang, Xu, et al., 2022). Briefly, the gelatin was dissolved by adding it to distilled water (solid: water ratio = 1:50, w/v) and stirring the mixture at 500 rpm and 45 °C for 45 min. Next, acid-hydrolyzed agar was added to the solution at a ratio of agar to gelatin of 1:1 (w/w), and the mixture was heated to 90 °C. The pH was adjusted to 9 using 1 mol/L NaOH, and the mixture was stirred at 500 rpm for 45 min. Then, the pH was adjusted to 7 with 1 mol/L HCl, and the reaction was immediately stopped by placing the mixture in ice.

2.4. Characterization of the MRPs

2.4.1. Fourier-transform infrared (FT-IR) spectroscopy

The freeze-dried samples were mixed with KBr at a mass ratio of 1:100 and pressed into a thin sheet at a pressure of 20 MPa for 3 min. The FT-IR spectrometer (Thermo Fisher Nicolet iS50, USA) was scanned at 25 °C with a resolution of 4 cm⁻¹ in the wave number range of 4000–500 cm⁻¹.

2.4.2. Nuclear magnetic resonance (NMR) spectroscopy

¹³C NMR analysis was performed by Bruker Avance 500 MHz high-resolution NMR spectrometer (Bruker 500, Germany). Samples were dissolved in DMSO-*d*₆ into a concentration of 50 mg/mL.

2.4.3. Ultraviolet absorption and fluorescence intensity

The freeze-dried powders were dispersed in distilled water (5 mg/mL). Their absorbance at 294 and 420 nm was determined by UV-Vis spectrometer (Thermo Fisher, Massachusetts, USA) to indicate the browning strength of the samples and the content of intermediate products (Aziznia et al., 2024). Distilled water was used as a blank. The fluorescence intensity of the sample was measured at the excitation wavelength of 347 nm with a fluorescence spectrophotometer (Cary Eclipse, Agilent, USA), and the emission spectrum was scanned in the range of 370–550 nm (Huang et al., 2022). The slit width for both excitation and emission was 5 nm.

2.4.4. Determination of free amino groups

The content of free amino groups was determined using the o-phthalaldehyde (OPA) method (Wang et al., 2021). The OPA reagent was prepared by dissolving 80 mg of OPA in 2 mL of ethanol and mixing it with 5 mL of 20 % (w/v) SDS solution, 50 mL of 0.1 mol/L sodium tetraborate solution, and 200 μ L of β -mercaptoethanol. Finally, the reagent was diluted to 100 mL with distilled water. The 200 μ L (2 mg/mL) sample solution was mixed with 4 mL of OPA reagent and reacted at

35 °C for 2 min. The absorbance at 340 nm was then measured. A calibration curve was obtained by using L-Leucine as a standard.

2.4.5. Contact angle

The wettability of the sample was evaluated using the drop contact angle method, as described by Xiao et al. (2023). A 1 % (w/v) solution of the sample was prepared in distilled water and dried to form a film at 40 °C. Next, 5 µL of distilled water was dropped onto the surface of the film using a micro syringe. The water contact angle of the sample was automatically recorded and calculated within 120 s using a contact angle tester (Innuo, CA100C, Shanghai, China).

2.5. Preparation of Pickering emulsions

Pickering emulsions were prepared using different concentrations of agar-gelatin powders (0.25–1.5 %) and soybean oil phase fractions (10–90 %). The agar-gelatin suspension was mixed with soybean oil in a beaker at ambient temperature using an NS-20 shaft high-speed stirrer (DLAB, D-160, Beijing, China) operating at 15,000 rpm for 120 s. The resulting emulsions were evaluated for stability and stored at ambient temperature.

2.6. Effect of environmental factors on the stability of Pickering emulsions

All emulsions were prepared using a fixed concentration of agar-gelatin powders 0.75 % and an oil fraction of 50 %. The stability of the emulsions was evaluated by replacing the aqueous phase with NaCl solutions of varying ionic strengths (0, 50, 75, 100, 150, 200, and 300 mmol/L). The pH stability of the Pickering emulsion was assessed by adjusting the pH of the agar-gelatin suspensions to 1, 3, 5, 7, 9, and 11 using NaOH or HCl at 25 °C. To evaluate the temperature stability of the emulsions, freshly prepared samples were incubated in a water bath at different temperatures (4 °C, 30 °C, 40 °C, 50 °C, 60 °C, 70 °C, 80 °C, and 90 °C) for 1 h.

2.7. Characterization of Pickering emulsion

2.7.1. Emulsifying properties analysis

The emulsion activity index (EAI) and emulsion stability index (ESI) were assessed based on the turbidity of the diluted emulsions (Pirestani et al., 2017; Zhang et al., 2021). 50 µL of freshly prepared emulsion was diluted to 10 mL by adding 0.1 % (w/v) SDS solution. The absorbance values of freshly prepared emulsions at 0 min and 10 min were obtained at 500 nm using a UV–Vis spectrometer (Thermo Fisher, Massachusetts, USA). EAI and ESI values were calculated as follows:

$$EAI(m^2/g) = \frac{2 \times 2.303 \times A_0 \times D}{C \times \emptyset \times L \times 10^4}$$

$$ESI(min) = \frac{A_0}{A_0 - A_{10}} \times 10$$

where A_0 and A_{10} are the absorbance of emulsions at 0 min and 10 min, respectively. D is the dilution factor, C is the initial concentration of powders, \emptyset is the oil volume fraction of the emulsion and L is the optical path.

2.7.2. Centrifugal stability

The emulsion in a scaled centrifuge tube was centrifuged at 3000 × g for 20 min. Phase separation was accelerated via centrifugation, producing an oil phase at the top, a cream phase in the middle, and an aqueous phase at the bottom.

2.7.3. Particle size and zeta-potential measurements

The droplet size distribution of the emulsion was measured by laser particle analyzer (Weina particle Instruments, Winner 2000, Jinan, China) with a detection range of 0.1 µm to 300 µm. The emulsions were

diluted 100 times with 1 % (w/w) sodium dodecyl sulfate (SDS) solution during particle size measurement to avoid multiple light scattering effects (Zhang, Wang, & Adhikari, 2022). The zeta-potential of emulsion was measured using a zeta-sizer Nano-ZS90 (Malvern Instruments, Worcestershire, Malvern, UK) after being diluted 100 times with distilled water. The measurements were performed at 25 °C and repeated three times for each sample.

2.7.4. Optical microscopy

The emulsions were diluted 20 times with distilled water, and the microstructure images of the emulsion were observed with an optical microscope (Motic, B1-220PL, China). All measurements were taken at 25 °C with a magnification of 100 times.

2.7.5. Confocal laser scanning microscopy

The microstructure of the emulsion was observed by a confocal laser scanning microscope (ZEISS, LSM 880 NLO, Oberkochen, Germany). Briefly, the mixed dye 100 µL (containing 1 mg/mL Nile red and 5 mg/mL Nile blue, dissolved in soybean oil and deionized water) was added to 1 mL freshly prepared emulsion for dyeing, and the slide was prepared after dyeing for 1 h. Subsequently, the sample was observed with the excitation and emission wavelengths set to 473 nm and 520 nm, 635 nm and 647 nm, respectively (Xiao, Chen, et al., 2022). The oil confidence signal was set to red, the continuous signal to blue, and the magnification was 400×.

2.7.6. Cryo-scanning electron microscopy (Cryo-SEM)

The surface morphology of the emulsions was observed using a cryo-scanning electron microscope (ThermoFisher, Helios G4 UC, Massachusetts, USA) with an acceleration voltage of 10 kV. The samples were frozen in liquid nitrogen (−196 °C). The frozen sample were cut with a cooled knife in a freezing separation chamber and sublimed at −80 °C for 40 min. After sublimation, the sample were sputter-coated with a gold-palladium alloy at 10 mA for 60 s and transferred to a Cryo-SEM to observe the structures.

2.8. Preparation and evaluation of low-fat mayonnaise

2.8.1. Preparation of mayonnaise

The preparation of mayonnaise was adapted from a previous report (Su et al., 2023). Briefly, 2 g of sugar and 2 g of salt were mixed with 15 g of egg yolks using a mixer (SUPOR, HB60A, Zhejiang, China) for 20 s. Subsequently, 75 g of soybean oil was slowly added to the mixture while mixing at 10,000 rpm for 5 min. Finally, 6 g of vinegar was added and stirred for 1 min to maintain the bright color of the mayonnaise. This process produced a full-fat mayonnaise with a fat content of 75 %, which was labeled as Full. To prepare low-fat mayonnaise, 5 % AGMs were used to replace some of the soybean oil during emulsification using the same method. These variants were labeled as AGMs 20 %, AGMs 40 %, AGMs 60 %, and AGMs 80 %, respectively.

2.8.2. Rheological properties of mayonnaise

The rheological properties of mayonnaise were measured using a DHR-1 rotational rheometer (TA Instruments, New Castle, USA). The test temperature was 25 °C, the diameter of the parallel geometry plates was 40 mm, and the plywood gap was set to 1000 µm. The strain was increased from 0.01 % to 10 % at a constant frequency of 1 Hz to determine the linear viscoelastic region (LVR) of the samples. In the LVR range, the constant strain was set at 0.1 %. Dynamic rheological tests were carried out in the angular frequency range of 0.1–100 rad/s to determine the energy storage modulus (G') and loss modulus (G'') of the samples. Steady state shear tests were carried out in the range of shear rate 0.1–100 s^{−1} to study the variation of apparent viscosity of the samples with shear rate. To study the thixotropic recovery of the samples, the samples were subjected to three shear scans (Choi et al., 2023), the first and third at a low shear rate of 0.1 s^{−1}, and the second at a high

shear rate of 10 s^{-1} , each lasting for 60 s. The thixotropic recovery rate of mayonnaise was calculated as follows:

$$\text{Recovery rate (\%)} = \frac{\text{Final viscosity in the 3rd section}}{\text{Initial viscosity}} \times 100$$

2.9. Statistical analysis

All experiments were repeated at least three times and the average was calculated. One-way ANOVA and Duncan's multiple range test were used to compare differences at a significant 5 % level using SPSS 17.0 software.

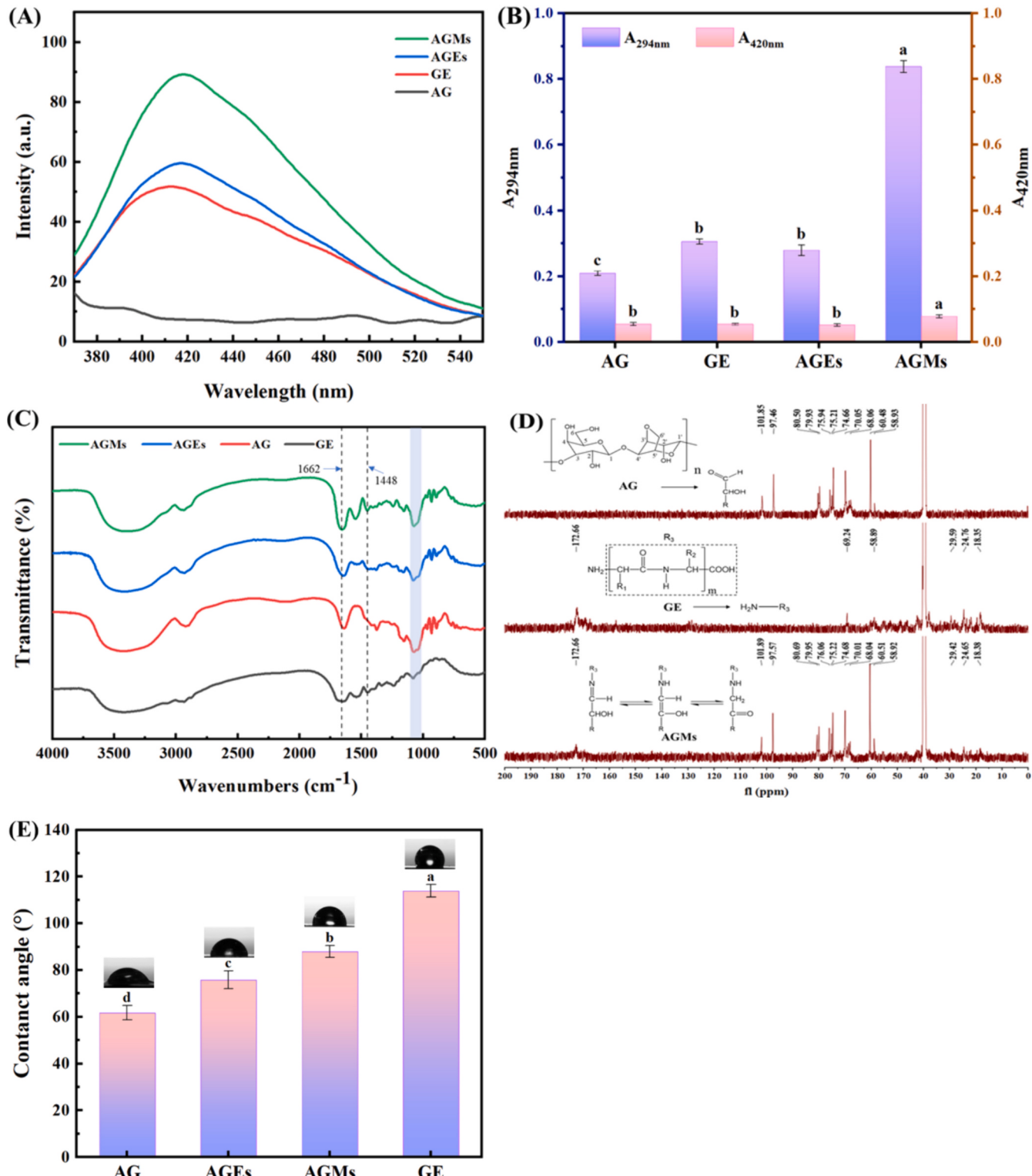


Fig. 1. Fluorescence spectra (A), UV absorptions at 294 nm and 420 nm indicate the degree of browning (B), FT-IR spectra (C), ¹³C NMR spectra (D), and contact angle (E) of AG, GE, AGEs, and AGMs. Different letters indicate significant differences at $p < 0.05$.

3. Results and discussion

3.1. Characterization of agar-gelatin Maillard products

3.1.1. Fluorescence intensity and ultraviolet absorption

The Maillard reaction generates fluorescent characteristic conjugates within the excitation wavelength range of 340–370 nm and emission wavelength range of 420–440 nm (Ni et al., 2021). Prior to the formation of melanoidins in the later stages of the Maillard reaction, the compounds produced in the initial phases of the reaction undergo cross-linking with adjacent amino acids or proteins, resulting in the formation of fluorescent polymer compounds (Liu, Li, et al., 2019). In Fig. 1A, it can be observed that under an excitation wavelength of 347 nm, AGMs exhibited the strongest fluorescence emission at 420 nm, with significantly higher fluorescence intensity compared to AGEs. This observation aligns with the typical fluorescent characteristics of substances generated through the Maillard reaction. Moreover, a blue shift was observed after the reaction when compared to gelatin, with the maximum emission wavelength shifting towards shorter wavelengths from 426 nm to 420 nm. These findings indicate the formation of distinct fluorescent molecules as a result of the Maillard reaction. A similar phenomenon was previously reported by Sun et al. (2023) during the covalent preparation of soybean meal hydrolysate with reducing sugars using the moist heat method.

The Maillard reaction is characterized by the generation of colored substances, and typically, the color intensity of the reaction products is positively correlated with the degree of browning. The degree of browning in the Maillard reaction can be quantified by measuring the absorbance of the reaction products at 420 nm, while the absorbance at 294 nm indicates the formation of intermediates (Cao et al., 2022). In Fig. 1B, it can be observed that the absorbance values of AGMs at 294 nm were significantly higher compared to the other three substances. This can be attributed to the thermal combination between the $\epsilon\text{-NH}_2$ group of gelatin and the -C=O group of acidolysis agar, resulting in the formation of Schiff bases. After undergoing Amadori rearrangement and degradation, small aldehyde or ketone molecules are formed as intermediates, which exhibit UV absorption at 294 nm. In the later stages of the reaction, these small molecular intermediates undergo various reactions such as cyclization, dehydration, and rearrangement, ultimately forming polymers with complex structures that exhibit light absorption at 420 nm. In our experimental conditions, there was no significant increase in absorbance at 420 nm for the AGMs, indicating that a majority of the reaction did not progress to the final stage.

3.1.2. Fourier-transform infrared (FT-IR) spectroscopy

The Maillard reaction results in the depletion of certain functional groups ($-\text{NH}_2$) and the generation of others (C=N , C=O , C-N), which often lead to changes in the FTIR spectra of the compounds involved (Fig. 1C). In the case of gelatin, the peaks observed around 1635 and 1541 cm^{-1} correspond to the amide I (C=O stretching) and amide II (N-H bending and C-N stretching) bands, respectively, which are characteristic of proteins (Wen et al., 2020). Upon conjugation with agar through the Maillard reaction, the amide I band of AGMs shifted to 1662 cm^{-1} , indicating the formation of Schiff bases and glycosylamine (early-stage products) that are typically produced during the Maillard reaction (Hou et al., 2024). The absorption peak corresponding to the O-H stretching vibration is typically observed in the range of 3000 to 3700 cm^{-1} . Upon introducing agar into gelatin, AGMs and AGEs exhibited broad absorption peaks in the 3000–3700 cm^{-1} range, indicating an increase in O-H groups compared to gelatin alone. Additionally, the conjugated AGMs displayed a new absorption peak at 1448 cm^{-1} , which can be attributed to the stretching vibration of the C-N bonds formed during the Maillard reaction (Cheng et al., 2022). The free amino group content of AGEs was 21.63 %, while that of AGMs was 15.35 % by the OPA method. This decrease could be attributed to the consumption of amino groups during the Maillard reaction, which was related to the

formation of C-N bonds. Agar itself exhibited characteristic absorption peaks in the 1000–1100 cm^{-1} range, which corresponded to the stretching of C-C , C-O , and the bending of C-H bonds. Interestingly, the absorption peak at 1000–1100 cm^{-1} for the conjugated AGMs was significantly enhanced, suggesting the presence of O-H group bending on the long chain covalently bonded to gelatin (Gao et al., 2024). These findings indicate the formation of a covalent bond between agar and gelatin through the Maillard reaction, resulting in a product with a characteristic structure incorporating both gelatin and agar.

3.1.3. Nuclear magnetic resonance (NMR) spectroscopy

To investigate the structural changes and chemical shifts of agar-gelatin following Maillard reaction, ^{13}C NMR spectroscopy was conducted. As depicted in Fig. 1D, both AG and AGMs exhibited two hetero head carbon signals within the range of 90 to 110 ppm. This observation suggests that the fundamental structure of agar consists of two monosaccharide units, namely $\beta\text{-D-galactose}$ and $\alpha\text{-L-galactose}$ (Zhang, Xiao, et al., 2023). It further indicates that AGMs still retain the basic structure of agar. The carbon signals associated with agarose were observed at C-1 (101.85 ppm), C-1' (97.46 ppm), C-2/2' to C-5/5' (68.00–80.50 ppm), C-6 (60.48 ppm), and C-6' (58.93 ppm). Compared to AG, AGMs exhibited a shift in their carbon signals towards lower fields, specifically at 101.89, 97.57, 80.69, 79.95, and 76.06 ppm. This shift can be attributed to the displacement caused by the generation of new functional groups resulting from the Maillard reaction (Tang et al., 2023). The carbon signals observed at 15–30 ppm corresponded to the amino acid side chains in gelatin. Additionally, the signal peak at 172.66 ppm indicated the presence of aldehyde acids, which corroborated previous findings (Tang et al., 2023). NMR analysis suggested that the fundamental structure of agar remained unchanged following the Maillard reaction, which aligns with the results obtained from FT-IR analysis.

3.1.4. Contact angle

The wettability of various particles can be determined by measuring the contact angle (θ), which allows for the evaluation of the Pickering emulsion type and the particles' emulsifying ability. Fig. 1E illustrates the contact angles of four different particles. AG exhibited a contact angle of only 61.7°, indicating its relatively high hydrophilicity. Upon the incorporation of gelatin, the contact angles of AGEs and AGMs particles increased to 75.8° and 87.9°, respectively. This increase suggests that the addition of gelatin to AG enhanced its surface hydrophobicity, which can be attributed to the amphiphilic nature of the gelatin molecules. The gelatin molecular chains tend to unfold, exposing more hydrophobic groups during the heating process of the reaction. It has been demonstrated that solid particles can be adsorbed on the oil-water interface to establish a stable particle adsorption layer under certain wettability conditions. This layer acts as a physical barrier, impeding droplet aggregation (Chen et al., 2023). When the contact angle (θ) is 90°, the particles are uniformly distributed in both oil and water phases, and the adsorption energy at the oil-water interface reaches a maximum, resulting in the optimal performance for Pickering emulsion stabilization (Liang et al., 2024). The contact angle of AGMs ($\theta = 87.9^\circ$) is closest to 90°, indicating superior emulsification capacity and a greater potential for Pickering emulsion stabilization.

3.2. Comparison of four different particle stabilization emulsions

To assess the potential of AGMs as Pickering emulsifiers, Pickering emulsions were prepared using AG, GE, AGEs, and AGMs as particulate emulsifiers. The emulsions had a concentration of 1 % particulate emulsifiers and an oil phase volume fraction of 50 %. The emulsification characteristics and storage stability of these four emulsions are presented in Fig. 2. In terms of storage stability, the emulsions formulated with AG displayed the poorest stability, as evidenced by significant oil precipitation and emulsion delamination after 7 days (Fig. 2A). Conversely, the emulsions prepared with AGMs exhibited the highest

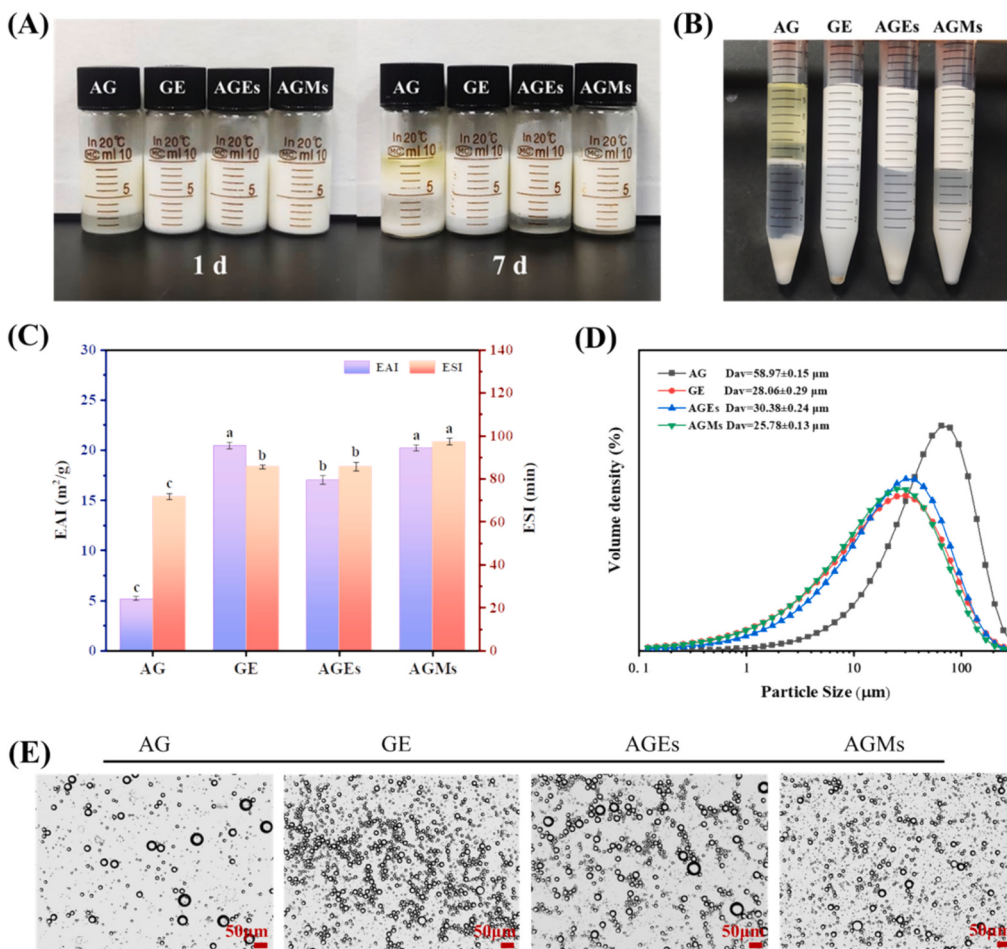


Fig. 2. Emulsions stabilized by four different particles AG, GE, AGES, AGMs. (A) Appearance photograph of emulsions stored for 1 and 7 days; (B) appearance photograph of emulsions after centrifugation at $3000 \times g$ for 20 min; (C) emulsion activity and emulsion stability of emulsions; (D) droplet size distribution of emulsions; (E) optical micrographs ($100\times$) of emulsion stored for 1 day, scale bar represents 50 μm . Different letters indicate significant differences at $p < 0.05$.

stability, with minimal changes in appearance during the storage period. These observations were reinforced by the emulsification activity (EAI) and emulsion stability (ESI) tests, which aligned with the centrifugal stability outcomes depicted in Fig. 2B. Optical microscope imaging revealed that the emulsions formulated with AG exhibited larger and more widely dispersed particle sizes (Fig. 2E). Conversely, the droplets stabilized by GE were smaller, denser, and clustered together, making them more prone to agglomeration and flocculation phenomena. This ultimately resulted in emulsion delamination and the formation of a turbid water layer. The droplets in the emulsions stabilized by AGES were noticeably uneven in size, although they were dispersed more evenly. In contrast, the droplets in AGMs-stabilized emulsions were uniformly sized and dispersed, representing the smallest particle size of the emulsion and demonstrating superior stability (Fig. 2C and D). Collectively, the emulsions prepared with AGMs powder exhibited the highest stability, underscoring AGMs' potential as Pickering emulsifiers. Additionally, the Maillard reaction significantly enhanced agar emulsification.

3.3. Stability of emulsions prepared with agar-gelatin Maillard products

3.3.1. Effect of AGMs concentration on emulsions stability

Fig. 3 illustrates the emulsions prepared using agar-gelatin powders at varying concentrations, after being preserved for 1 and 7 days. After 7 days of storage, no demulsification or oil leakage was observed in any of the emulsions, highlighting the potent emulsifying capacity of AGMs. As the particle concentration increased, the emulsion layer expanded,

droplet size decreased, and stability improved over time. When the particle concentration was below 1 %, the emulsion layer gradually increased with increasing particle concentration. In contrast, when the particle concentration exceeded 1 %, the emulsion layer's height remained constant. Furthermore, after 7 days of storage, the emulsion exhibited a non-flowing state and could be inverted, resembling an emulsion gel. These observations may be attributed to the insufficient adsorption of particles on the droplet surface at low particle concentrations, resulting in incomplete encapsulation of the droplets. As a means of minimizing the interfacial area, larger droplets formed. As the particle concentration increased, the droplet size decreased and became more uniform, signifying an increase in particle stability at the interface. Once a sufficient number of particles tightly adhered to the droplet surface, both droplet size and the height of the emulsion layer remained relatively unchanged. At high particle concentrations, particles completely covered the surface of all droplets, resulting in a thicker interface layer. This increased the spatial repulsion force and decreased the van der Waals attraction between droplets, effectively preventing aggregation and enhancing emulsion stability (Han et al., 2020). Furthermore, the increased number of particles adsorbed onto droplet surfaces raised the effective droplet density, reducing the density difference between the droplet and the continuous phase, which slowed down emulsion instability caused by gravity (Song et al., 2015). Additionally, higher particle concentrations elevated the viscosity of the continuous phase and could lead to the creation of a bridging network between droplets, impeding droplet movement and collisions, and thus promoting emulsion stability.

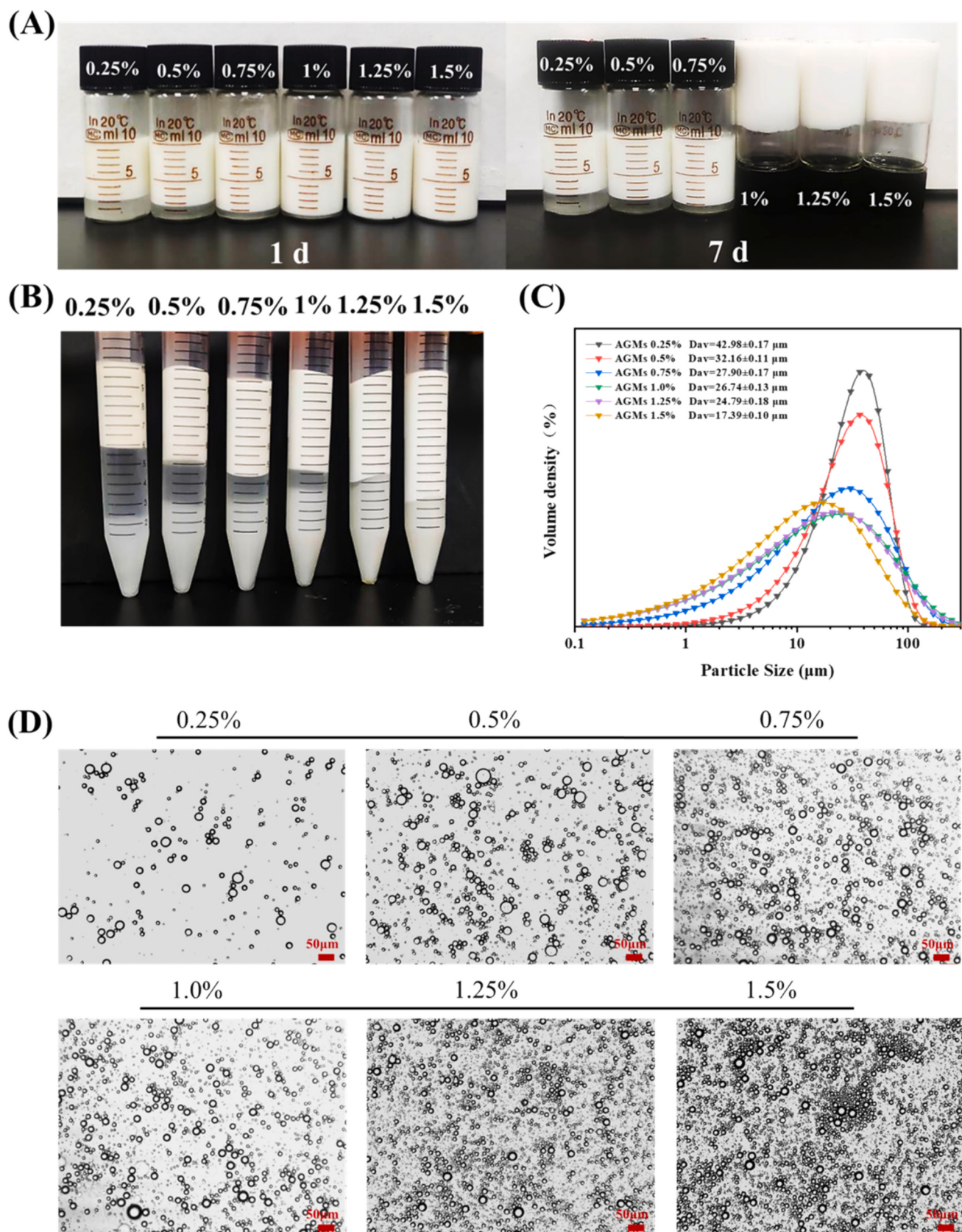


Fig. 3. Emulsions stabilized by agar-gelatin conjugates (AGMs) with different concentration. (A) Appearance photograph of emulsions stored for 1 and 7 days; (B) appearance photograph of emulsions after centrifugation at $3000 \times g$ for 20 min; (C) droplet size distribution of emulsions; (D) optical micrographs ($100\times$) of emulsion stored for 1 day, scale bar represents $50 \mu\text{m}$.

3.3.2. Effect of oil fraction on emulsions stability

The impact of varying oil phase contents (10 %–90 %) on the formation of Pickering emulsion using AGMs as stabilizer was investigated at a particle concentration of 0.75 % (w/v). As shown in Fig. 4, an O/W Pickering emulsion can be produced by increasing the oil phase content when the oil phase fraction is below 60 %, and no oil phase precipitation is observed even after 7 days of storage. Additionally, the height of the emulsion layer increases as the oil phase fraction increases, consistent with the results obtained from emulsion centrifugation. However, when the oil phase fraction exceeds 60 %, the emulsion takes on a slightly yellowish hue, and this phenomenon was consistently observed across repeated experiments, indicating that a stable emulsion cannot be formed under these conditions. Over time, nearly all of the oil leaked out and floated in the upper layer, while the emulsion layer and particles precipitated in the lower layer. These findings are consistent with those reported by Xiao et al. (2016), where approaching or surpassing the critical volume fraction of the internal oil phase in closely packed emulsion systems led to phase inversion and subsequent oiling off. Therefore, when the oil phase fraction exceeded 60 %, the AGMs at a concentration of 0.75 % (w/v) were unable to effectively adsorb onto the droplet surface and reduce surface tension. Microscopic observations also revealed that at oil phase fractions of 70 %–90 %, only a few droplets were formed, and there were noticeable particle aggregates.

3.3.3. Effect of pH on emulsions stability

Investigating the impact of different pH levels on the stability of emulsions is crucial for their application in food systems, considering the significant variation in the pH of the aqueous phase in food and beverage emulsions. As depicted in Fig. 5A, no noticeable variations in the morphology of the emulsions were observed under different water phase pH conditions. Even after 7 days of storage, the emulsion layer remained uniform and stable without any oil leakage. As the pH increased from 1 to 11, the zeta potential of the droplets decreased from +13.67 mV to -29.03 mV. This can be attributed to the protonation of AGMs at pH < pI and deprotonation at pH > pI. Previous studies have reported that when the zeta potential approaches zero and the pH is close to the isoelectric point, severe aggregation of whey isolate protein particles occurs (Wijaya et al., 2017), resulting in the poor stability of Pickering emulsions. Interestingly, at pH 3, the zeta potential approached 0 mV, yet the emulsion remained stable, suggesting that the primary mechanism responsible for stabilizing the emulsion was not electrostatic repulsion between droplets (Fig. 5D). It has been proposed that the stability of protein and polysaccharide conjugates in emulsions under different pH conditions is attributed to a shift from electrostatic repulsion to strong steric hindrance exerted by the conjugates (Caballero & Davidov-Pardo, 2021; Nooshkam et al., 2023). Additionally, an increase in the viscosity of the continuous phase also exhibited a certain enhancing effect on emulsion stability across different pH values. Optical microscope observations revealed no significant differences in the size and distribution of emulsion droplets at all pH values (Fig. 5E). Observations of the emulsion after centrifugation revealed that the emulsion layer at different pH values had the same height, indicating that pH has minimal impact on the stability of the emulsion formed by AGMs particles. Similar findings were reported by Chen et al. (2024), where emulsions stabilized solely by quinoa protein isolate (QPI) experienced flocculation and phase separation when the pH was close to the QPI isoelectric point. However, emulsions stabilized by a coupling of quinoa isolate protein and gum (QGUH) remained stable across the pH range. The difference in stability can be attributed to the limiting effect of the spatial repulsion of polysaccharide chain formation on droplet aggregation.

3.3.4. Effect of NaCl concentration on emulsions stability

Salt is a commonly used condiment in various foods, and NaCl, as a strong electrolyte, can dissociate into Na^+ and Cl^- ions in aqueous solutions, thereby influencing the surface charge of colloidal particles.

Therefore, it is important to investigate the impact of different ion concentrations on emulsion stability. The morphology of the emulsion at various ion concentrations (0–300 mM) is illustrated in Fig. 6. Comparing the emulsion state with and without the addition of NaCl (0 mM), there is virtually no difference. After 7 days of storage, no demulsification or oil separation occurred, and the appearance of the emulsion remained stable, as evidenced by the consistent height of the emulsion layer after centrifugation in Fig. 6B. This suggests that NaCl did not negatively affect the emulsion stability. Under optical microscope examination, it was observed that the droplet size was uniform and well-dispersed at low ion concentrations (<100 mM). However, when the NaCl concentration exceeded 100 mM, droplet aggregation became evident, leading to an increase in measured droplet size, as depicted in Fig. 6C. Nevertheless, as the NaCl concentration increased, the zeta potential of the emulsion rose from -23.9 mV to -12.3 mV, leading to a decrease in electrostatic repulsion between droplets. This phenomenon can explain the aggregation of droplets observed at higher NaCl concentrations. Previous research has indicated that a high concentration of ions in the aqueous phase hinders the electrostatic repulsion among particles, causing their accumulation at the droplet interface (Lu et al., 2018), which ultimately leads to emulsion instability. Although the addition of NaCl can reduce the zeta potential on the surface of the emulsion through electrostatic shielding, it is important to note that in certain NaCl concentration ranges, it can promote protein dissolution (Liu et al., 2021), cross-link protein particles to form a gel structure, and surround the droplets, thereby impeding phase separation of oil droplets. This may partially explain why the emulsions remained stable despite having a low absolute value of zeta potential. Additionally, the polysaccharide component of the agar-gelatin conjugate provides robust steric hindrance, thereby reducing the van der Waals attraction between droplets and weakening the instability of the emulsion induced by the reduced zeta potential. Previous studies have demonstrated that polysaccharide-protein conjugates can effectively enhance the salinity tolerance of emulsions, likely because of the improved electrostatic and steric repulsive forces (Pan et al., 2020). Therefore, the emulsion stabilized with AGMs powder exhibits remarkable salt tolerance and is well-suited for use in food systems with high salt content.

3.3.5. Effect of temperature on emulsions stability

As an important element of food processing technology, heat treatment has a significant impact on the structure and stability of emulsions. As depicted in Fig. 7, emulsion samples were subjected to different temperatures for 1 h to assess their thermal stability based on appearance and optical microscope images. All samples remained intact without any signs of oil leakage after being held at various temperatures for 1 h, and the same was true after storing them at room temperature for 7 days. However, at temperatures of 90 °C and 100 °C, a cloudy water layer appeared in the lower layer of the emulsions. Optical microscope observations demonstrated that there were no significant differences in droplet size or distribution when the temperature was below 80 °C, and uniform-sized droplets with even dispersion could be formed. However, emulsions subjected to temperatures exceeding 80 °C experienced significant changes, causing multiple droplets to clump together and resulting in flocculation. This phenomenon occurs because high temperatures accelerate the Brownian motion between droplets, leading to increased collisions and facilitating aggregation. However, the droplet structure remains intact, preventing emulsion leakage. A similar finding was reported by Pan et al. (2020) in their study on the physical stability of emulsions stabilized by Maillard products derived from whey protein hydrolysates and linear dextrans. Additionally, protein denaturation and polysaccharide molecular dissolution under high temperature conditions are key factors contributing to the instability of protein or polysaccharide Pickering particles. Conversely, emulsions stabilized by whey protein and lactose conjugates exhibit enhanced thermal stability at high temperatures, as reported by Liu, Wang, et al. (2019). The

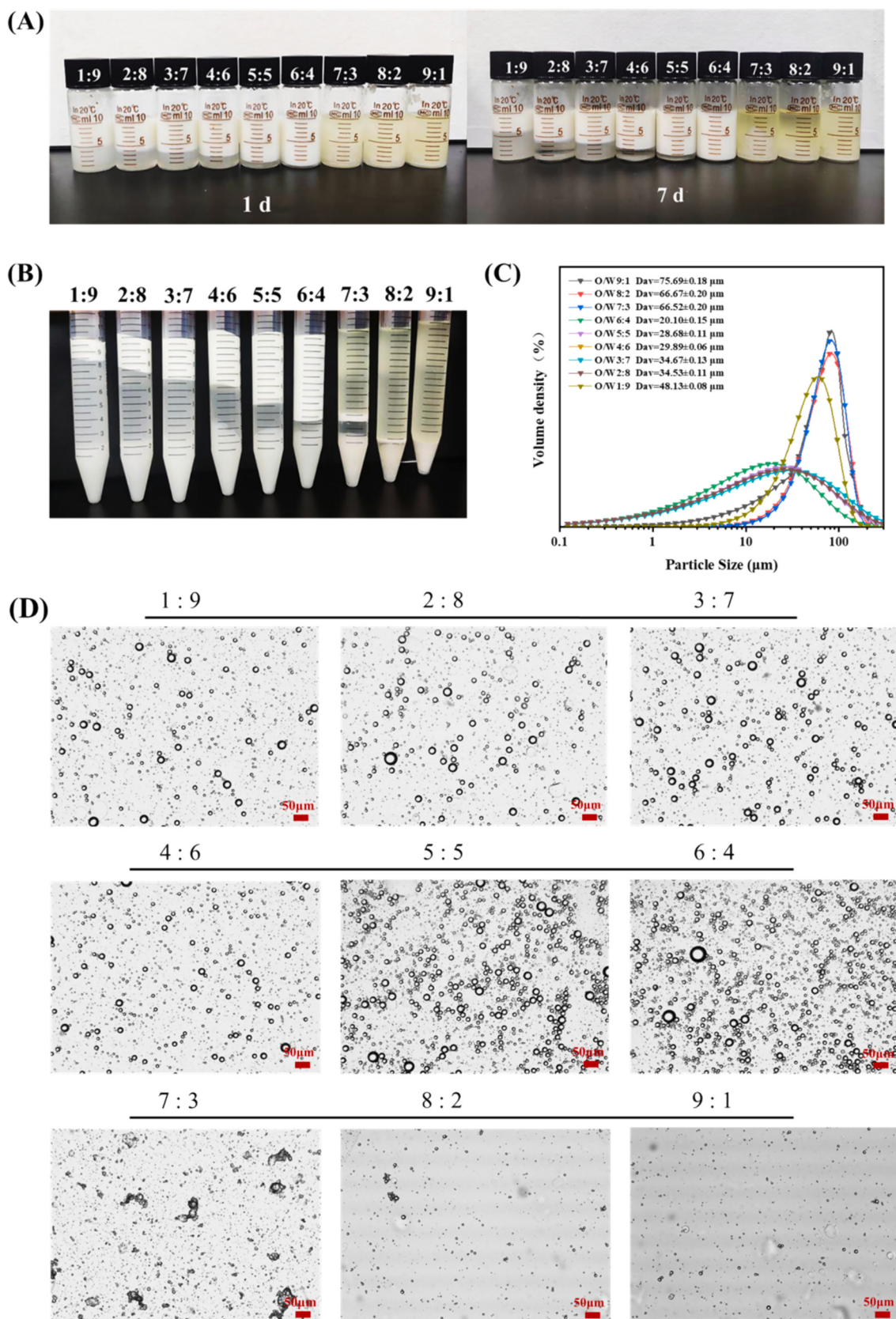


Fig. 4. Emulsions stabilized by agar-gelatin conjugates (AGMs) with different ratios of oil to water. (A) Appearance photograph of emulsions stored for 1 and 7 days; (B) appearance photograph of emulsions after centrifugation at $3000 \times g$ for 20 min; (C) droplet size distribution of emulsions; (D) optical micrographs ($100\times$) of emulsion stored for 1 day, scale bar represents $50 \mu\text{m}$.

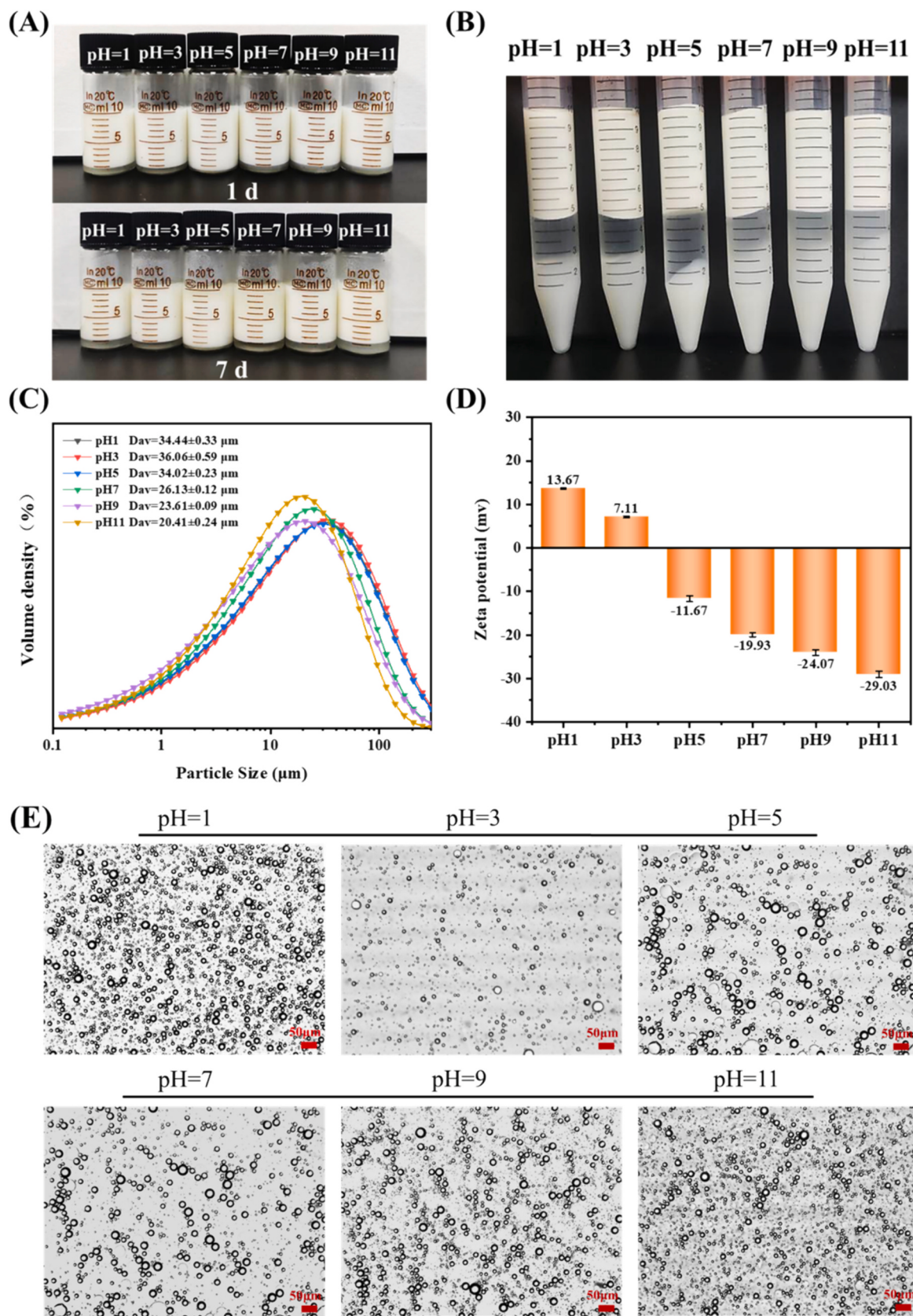


Fig. 5. Effect of pH on the stability of emulsions stabilized by agar-gelatin conjugates (AGMs). (A) Appearance photograph of emulsions stored for 1 and 7 days; (B) appearance photograph of emulsions after centrifugation at $3000 \times g$ for 20 min; (C) droplet size distribution of emulsions; (D) zeta potential of emulsions at different pH conditions. (E) Optical micrographs ($100\times$) of emulsion stored for 1 day, scale bar represent $50\text{ }\mu\text{m}$.

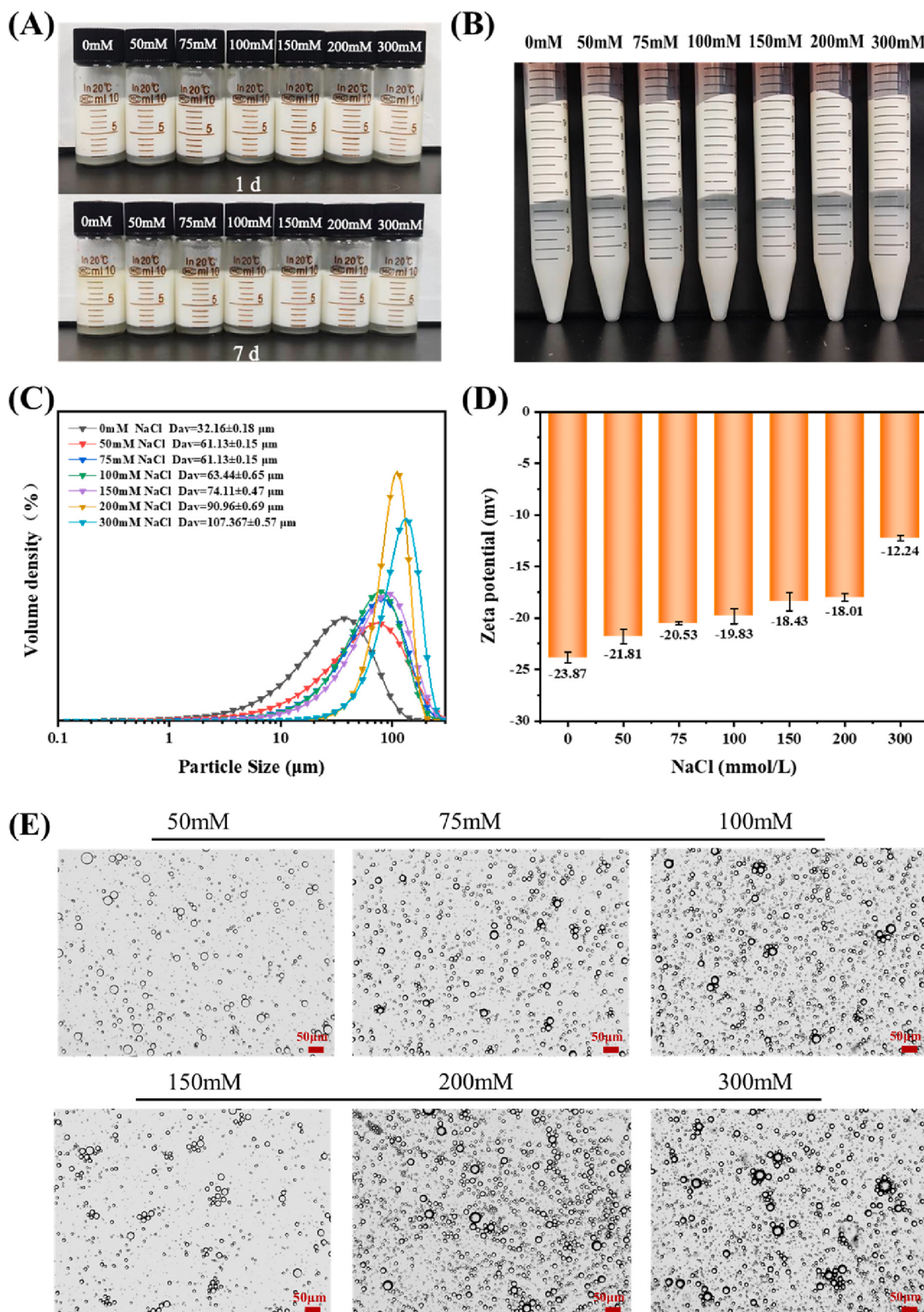


Fig. 6. Effect of NaCl concentration on the stability of emulsions. (A) Appearance photograph of emulsions stored for 1 and 7 days; (B) appearance photograph of emulsions after centrifugation at $3000 \times g$ for 20 min; (C) droplet size distribution of emulsions; (D) zeta potential of emulsions at different NaCl concentration. (E) Optical micrographs ($100\times$) of emulsion stored for 1 day, scale bar represent 50 μm .

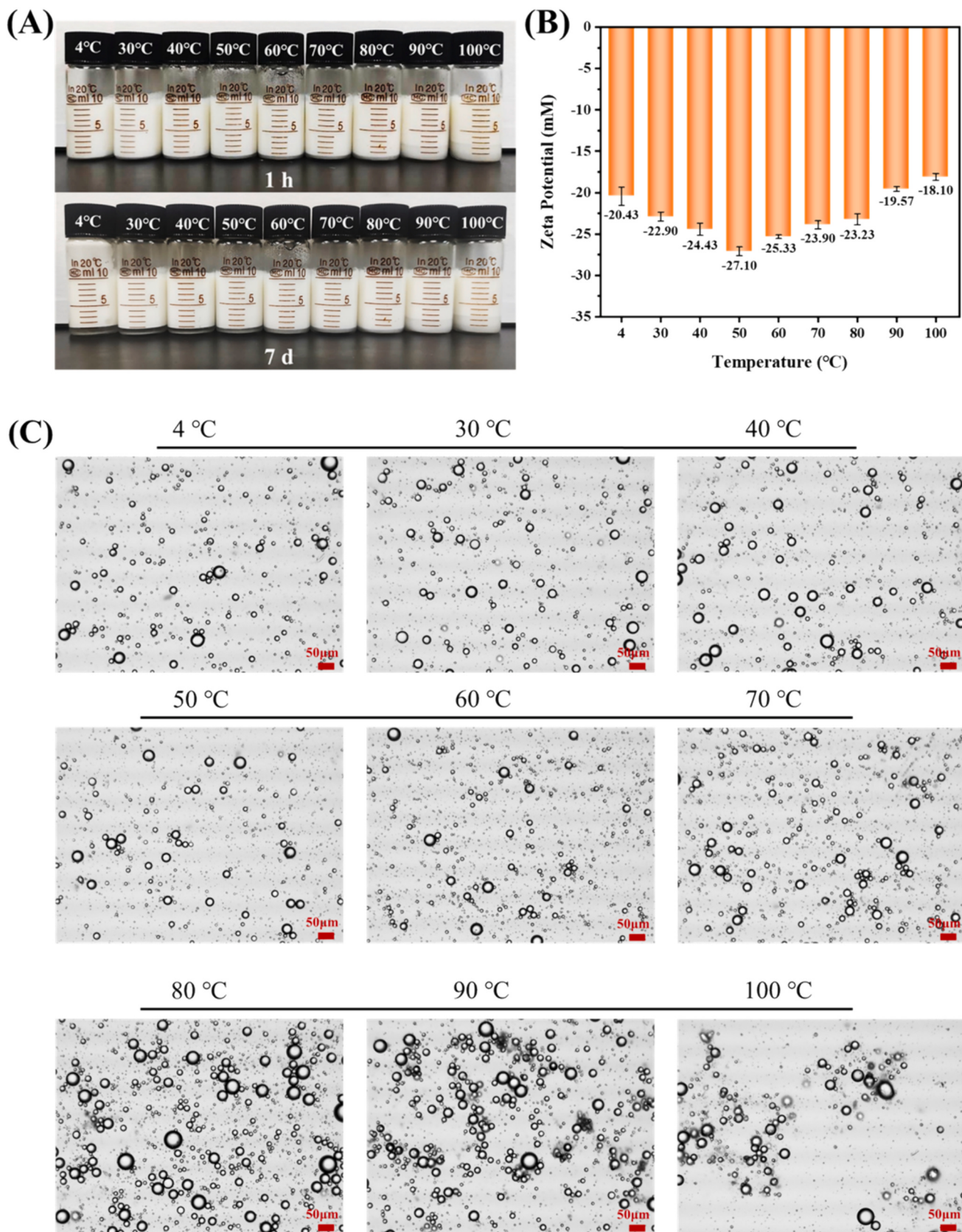


Fig. 7. Effect of different temperature on the stability of emulsions stabilized by agar-gelatin conjugates (AGMs). (A) Appearance photograph of emulsions treated for 1 h at different temperatures and stored for 7 days; (B) zeta potential of emulsions at different NaCl concentration. (C) Optical micrographs ($100\times$) of emulsions after 1 h treatment at different temperatures, scale bar represent 50 μm .

emulsions merge without compromising their structure due to the thicker interfacial layer provided by the conjugates, aligning with our own findings. Hence, emulsions stabilized by AGMs demonstrate exceptional thermal stability and can be employed in food systems that require heat processing.

3.4. Microstructure of emulsions

The CLSM was used to provide an intuitive way to illustrate the interfacial structure of Pickering emulsions fabricated by different particles, as shown in Fig. 8, where the red represents the oil phase and blue represents different particles. Obviously, the red oil phase is inside the

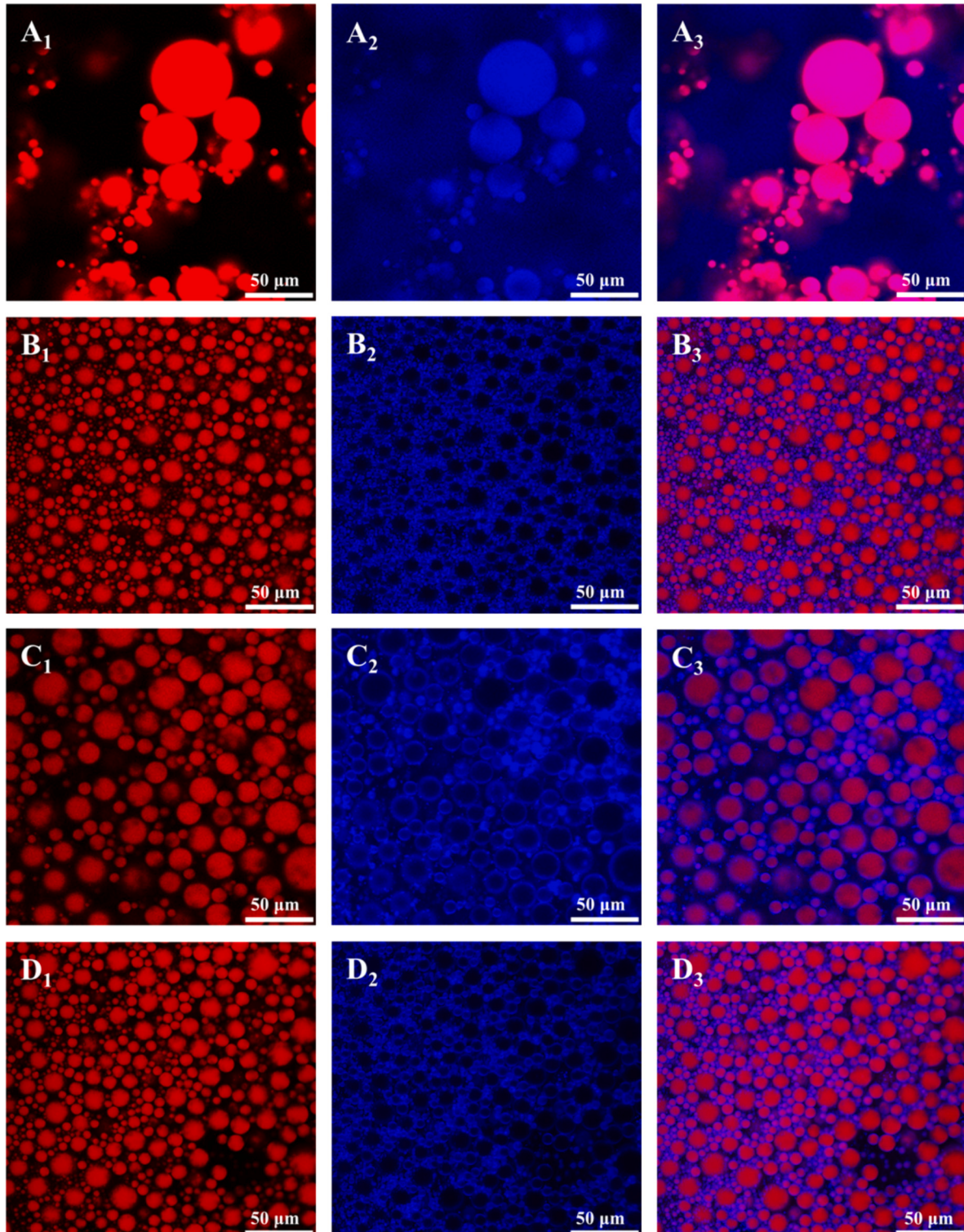


Fig. 8. Confocal laser scanning microscope images ($400\times$) of four different particle stabilized Pickering emulsions, scale bar represent $50\text{ }\mu\text{m}$. (A₁-A₃) AG particle stabilized emulsions; (B₁-B₃) GE particle stabilized emulsions; (C₁-C₃) AGEs particle stabilized emulsions; (D₁-D₃) AGMs particle stabilized emulsions. Oil phase was shown in red (A₁-D₁), water phase was shown in blue (A₂-D₂), combined images of oil phase and water phase (A₃-D₃).

droplet and the blue particles form a dense stacking layer at the droplet boundary, forming a dense spatial barrier that can effectively prevent the aggregation and Ostwald maturation of the droplets, thus maintaining the stability of the emulsions, and the Pickering emulsions prepared were all typical O/W systems. The limited emulsification properties of the agar particles resulted in an unstable emulsion that showed oil leakage, which was demonstrated in Fig. 2A. As a result, overlapping of the two dyes and irregularly shaped droplets were observed in Fig. 8(A₁–A₃). The emulsion droplets stabilized by GE particles were small and dense. Most of the droplets shared a common interfacial film to bridge, with the particles filling the space between the droplets randomly (Fig. 8B₂). As shown in Fig. 8C₂ and D₂, a distinct interface layer could be observed around the emulsion droplets stabilized by AGEs and AGMs. There were particles adsorbed on the surface of the oil droplet, with some additional free not adsorbed particles observed clearly in Fig. 8C₃, while a tight interfacial layer around the oil droplet with no visible unabsorbed particles in Fig. 8D₃. This was consistent with the phenomenon shown in Fig. 2A, where AGEs particles that were not adsorbed on the surface of the oil droplet were deposited at the bottom because the effect of gravity.

To understand the stabilizing mechanism of the Pickering emulsions by the four particles, the microstructure of the emulsions was observed by cryo-SEM (Fig. 9). The emulsion formed by AG had filamentary connections between droplets, and a small amount of filamentary material adhered to the surface of the droplets, which had not enough interfacial film and spatial positional resistance, so the emulsions could not be stabilized well. The emulsion droplets stabilized by GE were stacked tightly due to the thick accumulation and covering of gelatin. The emulsion formed by AGEs mainly rely on the weak gel network formed during the emulsification process and the filling of gelatin in the pores to stabilize the emulsion, since gelatin was prone to absorb water and dissolve thus there was aggregation in the continuous phase of the emulsion. The emulsion stabilized by AGMs mainly rely on the weak gel network structure formed between the droplets during the emulsification process to stabilize the emulsions.

To explore the mechanism of weak gel network formation between droplets, the same homogenization treatment was performed on four different particle suspensions without oil phase. The aim was to determine whether the particles would self-assemble to form a weak gel network structure during high-speed shear force and energy input. The results shown that none of them were able to form a network in the absence of oil, and the particles settled quickly in the lower layer, leaving a clear water layer on top after homogenization (Fig. 9E). The network structure was present in the system only when the oil phase was added. This may be due to the oil droplets inducing the AGMs particles to self-assemble to form a weak gel network during the emulsification process, limiting the movement of droplets. Xiao, Chen, et al. (2022) had discovered irregular networks in Pickering emulsions prepared by hexanoylated agar microgels and suggested that the self-assembled network through the microgels played a more significant role in the system. While octenyl succinylated agar microspheres could not form a gel network structure but only adsorbed on the oil-water interface in a multi-layer aggregate or single-layer bridge structure (Chen et al., 2023). Based on the special swelling and gelation properties of agar, this difference may be caused by the varying morphology of particles. The irregular agar microgels and powders were adsorbed on the surface of the oil droplets during emulsification and gradually absorbed water and swell in the system. The concentration of particles on the contact surface increased with the increase of the contact area between particles. It is widely acknowledged that when the concentration of the polymer exceeds a critical value, the attractive force may dominate the repulsive force (Ye et al., 2020). The attraction between particles could promote the formation of gel networks. Spheres have the smallest specific surface area among all object forms, resulting in the smallest contact area for the same mass. When considering agar microspheres, their spherical shape meant that there was at most one point of contact between them. This

limited contact between particles resulted in insufficient attraction to form a gel network. Whereas, the morphology of powders was irregular in this study, allowing the networks to form between droplets. Because of the weak interaction forces (electrostatic and van der Waals forces) present between the mixture of agar and gelatin, AGEs formed a loosely absorbed and disordered network structure around droplets, with some particles unabsorbed (Figs. 8C and 9C). The Maillard conjugates of agar and gelatin were bound by covalent bonds, and electrostatic attraction occurred between them due to the presence of amino and sulfuric acid groups. Therefore, AGMs formed a regular network and tightly attached to oil droplets (Figs. 8D and 9D), playing an important role in emulsion stabilization.

In conclusion, AGMs formed the most stable emulsions. The CLSM and the Cryo-SEM results provided insights that the particles forming a dense interfacial layer at the droplet boundary and meanwhile self-assembled to form a network structure prompted by oil droplets responsible for sustaining and stabilizing the emulsions.

3.5. Rheological properties of mayonnaise prepared with agar-gelatin Maillard products

To further assess the feasibility of producing low-fat mayonnaise using AGMs, rheological tests were conducted and compared with commercially available BYS mayonnaise and homemade full-fat mayonnaise. The oscillatory frequency measurements of the mayonnaises are shown in Fig. 10A and B. All mayonnaise samples exhibited frequency-dependent increases in both G' and G'', indicating weak gel properties. Furthermore, the G' values were higher than the G'' values within the linear viscoelastic region (LVR), suggesting that all samples displayed solid-like behavior resembling conventional mayonnaise. Typically, reducing the fat content in mayonnaise would result in a transition from a solid-like state to a more liquid consistency, impacting the texture. However, the low-fat mayonnaise prepared with AGMs, a Maillard product, maintained the viscoelastic properties of traditional mayonnaise. This can be attributed to the unique gelation behavior of AGMs, which form an ordered network structure and preserve the solid-like state of the mayonnaise even at low lipid content. Moreover, compared to commercial BYS, the low-fat mayonnaise exhibited a lower energy storage modulus (G'), indicating slightly lower gelation properties than the commercial control samples. It has been documented that samples with higher oil content typically have higher G' values as well (Yalmanci et al., 2023). The steady shear properties of the mayonnaise samples are presented in Fig. 10C, where viscosity decreased with increasing shear rate. Under applied shear forces, all samples exhibited shear-thinning flow characteristics, which is typical behavior for mayonnaises (Yalmanci et al., 2023). This behavior can be attributed to the collapse of intermolecular interactions and connections between droplets during shearing. Intriguingly, homemade mayonnaise displayed the same flow behavior as commercial BYS mayonnaise, but its overall viscosity was slightly lower than that of BYS. This could be linked to the addition of edible colloids such as xanthan gum or guar gum as thickeners in commercial mayonnaise. Among all the substitution levels, AGMs 60 % exhibited the lowest viscosity, while the viscosity of AGMs 80 % increased again, suggesting that adding large amounts of AGMs helped to maintain the viscosity of the mayonnaise. This may be related to the gel network structure formed by AGMs. The three-dimensional network structure hinders the movement of oil droplets and maintains the elastic morphology of the mayonnaise (Heggset et al., 2020). Therefore, AGMs 80 % also has a higher elastic modulus (G') than AGMs 60 %. At lower substitution levels, the viscosities of AGMs 20 % and AGMs 40 % were similar to that of full-fat mayonnaise. However, AGMs 20 % showed a faster rate of viscosity decrease with increasing shear rate. As the oil content was reduced and not much AGM was added, there was neither enough oil to maintain the viscosity of the system nor more AGMs to form a gel network. Both the oil and AGMs have a promoting effect on the gel structure of mayonnaise (Gu et al., 2016). With

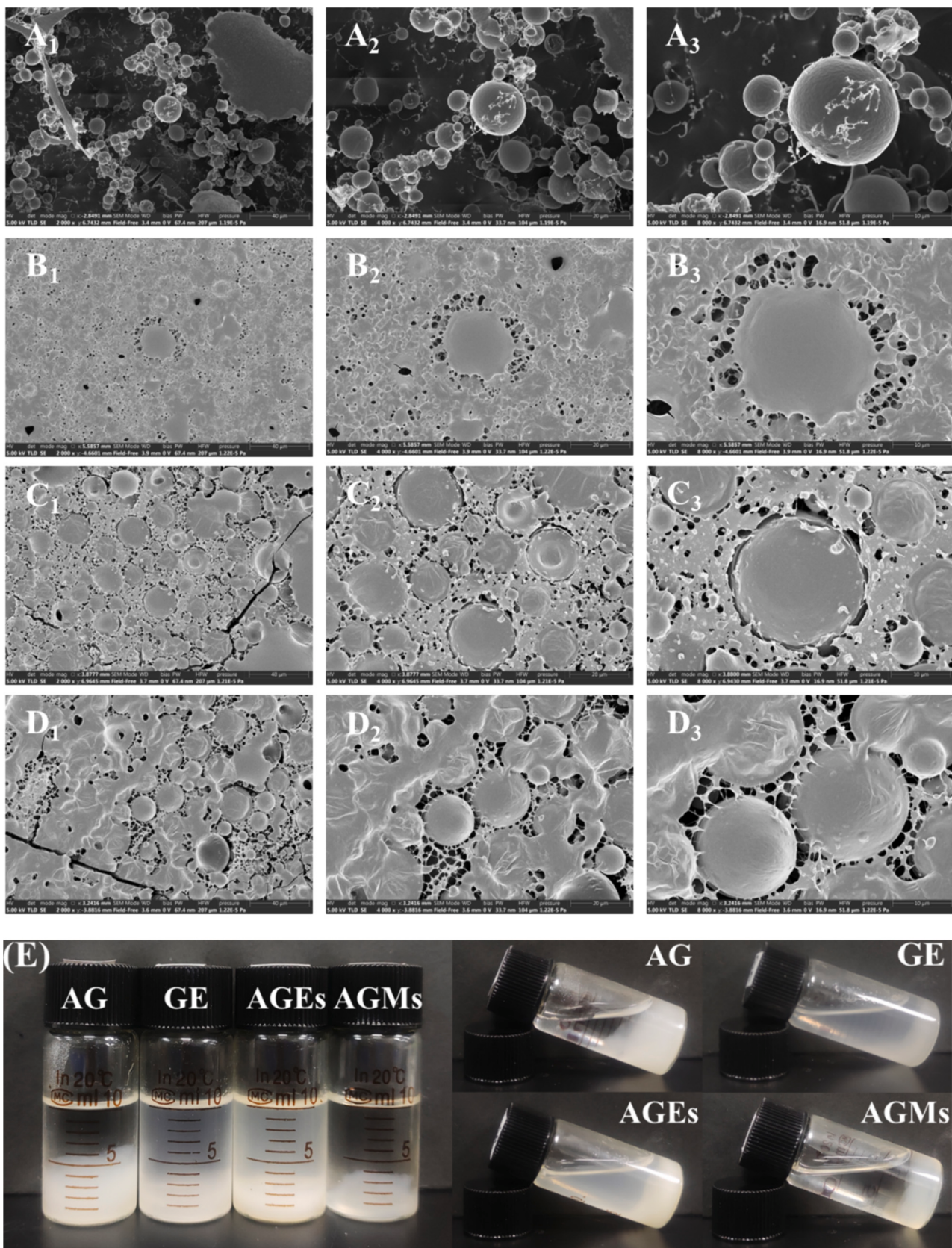


Fig. 9. The oil droplet surfaces of four different particle-stabilized Pickering emulsions observed by cryo-SEM (A-D), the appearance of four different particles after water phase homogenization (E). (A₁-A₃) AG particle stabilized emulsions; (B₁-B₃) GE particle stabilized emulsions; (C₁-C₃) AGEs particle stabilized emulsions; (D₁-D₃) AGMs particle stabilized emulsions. Scale bar in photos represent 40 µm (left), 20 µm (center), and 10 µm (right), respectively. The magnification times in photos represent 2000 × (left), 4000 × (center), and 8000 × (right), respectively.

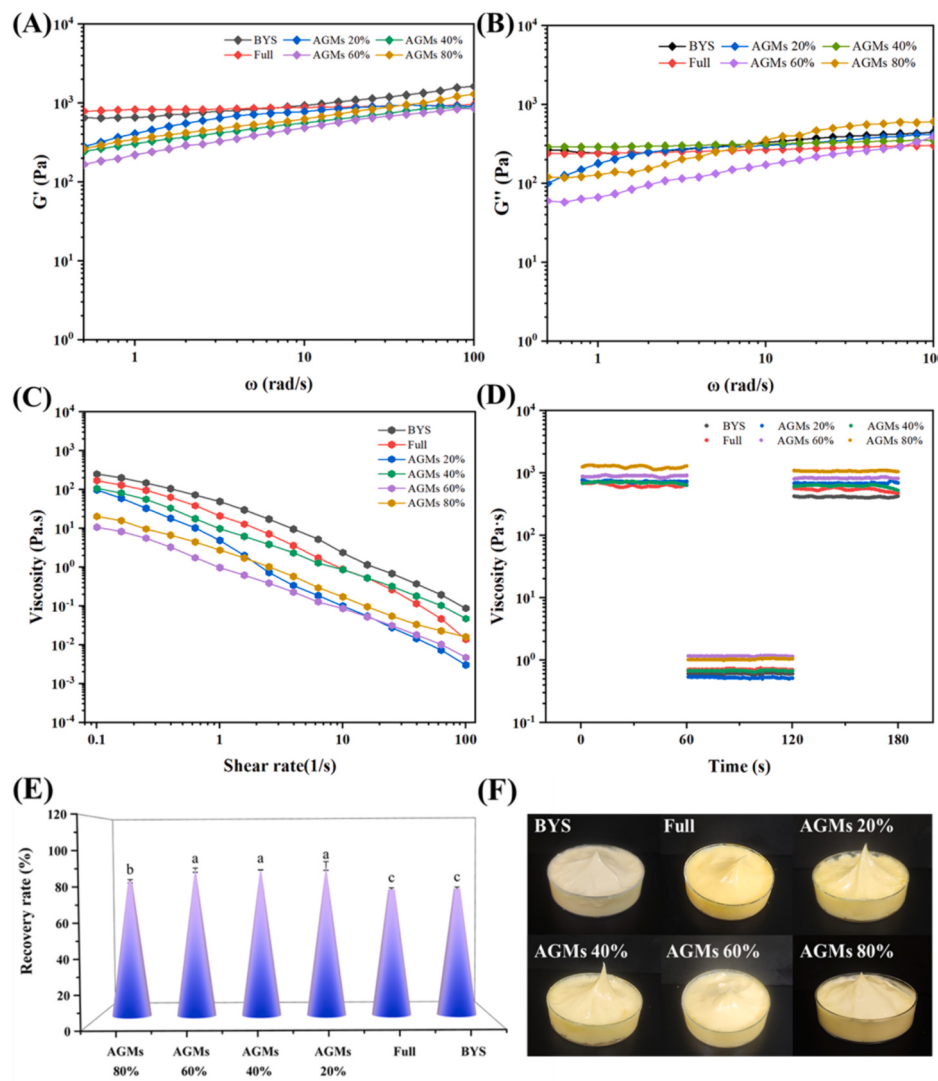


Fig. 10. (A) Variation of G' in frequency; (B) variation of G'' in frequency; (C) relationship between shear stress and apparent viscosity; (D) thixotropic tests; (E) recovery rate; (F) visual appearance of mayonnaise. BYS denote commercial mayonnaise, Full denote homemade mayonnaise, AGMs denote low-fat mayonnaise, and 20 %–80 % represent different levels of substitutes, respectively.

the addition of fat substitutes, the oil content reduces, while the AGMs increases in mayonnaise. As a result, different oil-AGMs ratios will be generated, showing the different states of mayonnaise.

Mayonnaise, being a spreadable sauce, undergoes multiple sudden deformations during consumption, leading to a weakening of its viscoelastic solid properties. Therefore, the ability to recover its structure is a crucial indicator for assessing mayonnaise quality. The 3-ITT (Instantaneous Time Test) is an important evaluation that examines the impact of sudden forces or deformations on the rheological properties of food products. It simulates everyday movements like shaking and squeezing that food items experience (Toker et al., 2015). Fig. 10D illustrates how the viscosity of the mayonnaise samples changes with the applied shear rate at different time intervals. In the first stage, at a low shear rate of 0.1 s^{-1} , the viscosity of all samples remained essentially constant. However, in the second stage, when subjected to a sudden increase in shear rate to 10 s^{-1} , the structure of the mayonnaise was disrupted, leading to a significant decrease in viscosity. Upon reverting back to the lower shear rate of 0.1 s^{-1} in the third stage, the viscosity of the samples quickly recovered, indicating their ability to return to their original state after the applied deformation was removed. It has been reported that recovery rates higher than 70 % indicate excellent recovery properties

(Patel & Dewettinck, 2015). The thixotropic recovery rate is presented in Fig. 10E, demonstrating that all samples exhibited excellent thixotropic properties. Furthermore, the low-fat mayonnaise prepared with AGMs exhibited a notable increase in the recovery rate. This suggests that the addition of Maillard products enhances the viscoelasticity of mayonnaise and aids in restoring the gel network that may have been damaged by external forces. In comparison to commercial products BYS and homemade full-fat mayonnaise, it exhibits superior structure retention capabilities. Overall, the results demonstrate that low-fat mayonnaise prepared with the Maillard product AGMs exhibited similar rheological properties or even better thixotropic reversibility than commercially available mayonnaise and homemade full-fat mayonnaise, indicating the potential to achieve the desired texture in low-fat mayonnaise.

4. Conclusion

This study introduces a safe and simple method for preparing Pickering emulsifiers AGMs, which are obtained by a Maillard reaction with agar and gelatin. The agar is acidified in the presence of hydrochloric acid, exposing its reducing ends and thereby successfully undergoing a

Maillard reaction with the free amino groups in gelatin under heated conditions. The synthetic route is safe and environmentally friendly as the use of organic solvents is avoided. Compared to agar or gelatin alone and their mixtures, emulsion droplets prepared with AGMs are smaller and more stable, and AGMs particles exhibit better emulsification capacity. Laser confocal and cryo-electron microscopy observations revealed that AGMs powders can be directly used as solid emulsifiers to prepare typical O/W Pickering emulsions. The interfacial layer of particles and spatial site resistance synergistically enhance the physical stability of the emulsions. The low-fat mayonnaise prepared using AGMs is very similar to commercial mayonnaise in appearance and rheological behavior, demonstrating the potential application of AGMs in complex food systems. In conclusion, a Pickering emulsifier based on agar and gelatin is developed through the Maillard reaction, which provides a new direction for their application in food sectors. However, other organoleptic characteristics such as texture and flavor should be taken into account for further industry applications.

CRediT authorship contribution statement

Lipeng Du: Writing – review & editing, Writing – original draft, Investigation, Data curation. **Yi Ru:** Methodology, Formal analysis. **Huifen Weng:** Project administration. **Yonghui Zhang:** Software, Methodology. **Jun Chen:** Validation, Supervision. **Anfeng Xiao:** Supervision, Funding acquisition. **Qiong Xiao:** Writing – review & editing, Writing – original draft, Supervision, Funding acquisition, Conceptualization.

Declaration of competing interest

The authors declare that they have no known competing financial interests or personal relationships that could have appeared to influence the work reported in this paper.

Data availability

Data will be made available on request.

Acknowledgments

This work was supported by the National Natural Science Foundation of China: 32201941; National Natural Science Foundation of China: 22278173; Fujian Province Natural Science Foundation of China: 2021J01834; Fujian Province Natural Science Foundation of China: 2021J01836; Startup Research Fund of Jimei University: ZQ2020029.

References

- Abdul Khalil, H. P. S., Lai, T. K., Tye, Y. Y., Rizal, S., Chong, E. W. N., Yap, S. W., ... Paridah, M. T. (2018). A review of extractions of seaweed hydrocolloids: Properties and applications. *Express Polymer Letters*, 12(4), 296–317. <https://doi.org/10.3144/expresspolymlett.2018.27>
- Aminikhah, N., Mirmoghadaie, L., Shoaee-Aliabadi, S., Khoobakht, F., & Hosseini, S. M. (2023). Investigation of structural and physicochemical properties of microcapsules obtained from protein-polysaccharide conjugate via the Maillard reaction containing *Satureja khuzestanica* essential oil. *International Journal of Biological Macromolecules*, 252, Article 126468. <https://doi.org/10.1016/j.ijbiomac.2023.126468>
- Aziznia, S., Askari, G., Enamdjomeh, Z., & Salami, M. (2024). Effect of ultrasonic assisted grafting on the structural and functional properties of mung bean protein isolate conjugated with maltodextrin through maillard reaction. *International Journal of Biological Macromolecules*, 254, Article 127616. <https://doi.org/10.1016/j.ijbiomac.2023.127616>
- Caballero, S., & Davidov-Pardo, G. (2021). Comparison of legume and dairy proteins for the impact of Maillard conjugation on nanoemulsion formation, stability, and lutein color retention. *Food Chemistry*, 338, Article 128083. <https://doi.org/10.1016/j.foodchem.2020.128083>
- Cao, J., Yan, H., & Liu, L. (2022). Optimized preparation and antioxidant activity of glucose-lysine Maillard reaction products. *LWT - Food Science and Technology*, 161, Article 113343. <https://doi.org/10.1016/j.lwt.2022.113343>
- Chen, H., Chen, F., Xiao, Q., Cai, M., Yang, Q., Weng, H., & Xiao, A. (2021). Structure and physicochemical properties of amphiphilic agar modified with octenyl succinic anhydride. *Carbohydrate Polymers*, 251, Article 117031. <https://doi.org/10.1016/j.carbpol.2020.117031>
- Chen, K., Zhang, M., Wang, D., Mujumdar, A. S., & Deng, D. (2024). Development of quinoa (*Chenopodium quinoa* Willd) protein isolate-gum Arabic conjugates via ultrasound-assisted wet heating for spice essential oils emulsification: Effects on water solubility, bioactivity, and sensory stimulation. *Food Chemistry*, 431, Article 137001. <https://doi.org/10.1016/j.foodchem.2023.137001>
- Chen, W., Wang, W., Guo, M., Li, Y., Meng, F., & Liu, D. (2022). Whey protein isolate-gum Acacia Maillard conjugates as emulsifiers for nutraceutical emulsions: Impact of glycation methods on physicochemical stability and in vitro bioaccessibility of β-carotene emulsions. *Food Chemistry*, 375, Article 131706. <https://doi.org/10.1016/j.foodchem.2021.131706>
- Chen, Z., Xu, Y., Xiao, Z., Zhang, Y., Weng, H., Yang, Q., Xiao, Q., & Xiao, A. (2023). A novel Pickering emulsion stabilized by rational designed agar microsphere. *LWT - Food Science and Technology*, 181, Article 114751. <https://doi.org/10.1016/j.lwt.2023.114751>
- Cheng, Y.-H., Mu, D.-C., Feng, Y.-Y., Xu, Z., Wen, L., Chen, M.-L., & Ye, J. (2022). Glycosylation of rice protein with dextran via the Maillard reaction in a macromolecular crowding condition to improve solubility. *Journal of Cereal Science*, 103, Article 103374. <https://doi.org/10.1016/j.jcs.2021.103374>
- Choi, H. W., Ham, S. H., Hahn, J., & Choi, Y. J. (2023). Developing plant-based mayonnaise using pea protein-xanthan gum conjugates: A maillard reaction approach. *LWT - Food Science and Technology*, 185, Article 115137. <https://doi.org/10.1016/j.lwt.2023.115137>
- Feng, J., Berton-Carabin, C. C., Fogliano, V., & Schröén, K. (2022). Maillard reaction products as functional components in oil-in-water emulsions: A review highlighting interfacial and antioxidant properties. *Trends in Food Science & Technology*, 121, 129–141. <https://doi.org/10.1016/j.tifs.2022.02.008>
- Gao, K., Xu, Y., Rao, J., & Chen, B. (2024). Maillard reaction between high-intensity ultrasound pre-treated pea protein isolate and glucose: Impact of reaction time and pH on the conjugation process and the properties of conjugates. *Food Chemistry*, 434, Article 137486. <https://doi.org/10.1016/j.foodchem.2023.137486>
- Gu, J., Xin, Z., Meng, X., Sun, S., Qiao, Q., & Deng, H. (2016). A “reduced-pressure distillation” method to prepare zein-based fat analogue for application in mayonnaise formulation. *Journal of Food Engineering*, 182, 1–8. <https://doi.org/10.1016/j.jfooodeng.2016.01.026>
- Han, Y., Cheng, Z., Zhang, Y., Zhang, N., Zhu, X., Chen, X., Shao, Y., Cheng, Y., Wang, C., Luo, Y., Zhu, L., Xie, J., Wang, C., & Huang, Y. (2020). Effect of metal ions and pH on the emulsifying properties of polysaccharide conjugates prepared from low-grade green sea. *Food Hydrocolloids*, 102, Article 105624. <https://doi.org/10.1016/j.foodhyd.2019.105624>
- Heggset, E. B., Aaen, R., Veslum, T., Henriksson, M., Simon, S., & Syverud, K. (2020). Cellulose nanofibrils as rheology modifier in mayonnaise – A pilot scale demonstration. *Food Hydrocolloids*, 108, Article 106084. <https://doi.org/10.1016/j.foodhyd.2020.106084>
- Hou, S., Lai, C., Song, Y., Wang, H., Ni, J., & Tan, M. (2024). A food-grade and senescent cell-targeted fisetin delivery system based on whey protein isolate-galactooligosaccharides Maillard conjugate. *Food Science and Human Wellness*, 13(2), 688–697. <https://doi.org/10.26599/FSHW.2022.9250058>
- Huang, C., Cui, H., Hayat, K., Zhang, X., & Ho, C.-T. (2022). Variation of moisture state and taste characteristics during vacuum drying of Maillard reaction intermediates of hydrolyzed soybean protein and characterization of browning precursors via fluorescence spectroscopy. *Food Research International*, 162, Article 112086. <https://doi.org/10.1016/j.foodres.2022.112086>
- Huang, T., Tu, Z., Zou, Z., Shangguan, X., Wang, H., & Bansal, N. (2020). Glycosylated fish gelatin emulsion: Rheological, tribological properties and its application as model coffee creamers. *Food Hydrocolloids*, 102, Article 105552. <https://doi.org/10.1016/j.foodhyd.2019.105552>
- Kan, X., Chen, G., Zhou, W., & Zeng, X. (2021). Application of protein-polysaccharide Maillard conjugates as emulsifiers: Source, preparation and functional properties. *Food Research International*, 150, Article 110740. <https://doi.org/10.1016/j.foodres.2021.110740>
- Kim, Y. J., Yong, H. I., Chun, Y. G., Kim, B.-K., & Lee, M. H. (2024). Physicochemical characterization and environmental stability of a curcumin-loaded Pickering nano emulsion using a pea protein isolate-dextran conjugate via the Maillard reaction. *Food Chemistry*, 436, Article 137639. <https://doi.org/10.1016/j.foodchem.2023.137639>
- Liang, W., Deng, F., Wang, Y., Yue, W., Hu, D., Rong, J., Liu, R., Xiong, S., & Hu, Y. (2024). Interfacial behavior and micro-rheological performance of Pickering emulsions co-stabilized by β-cyclodextrin and xanthan gum. *Food Hydrocolloids*, 149, Article 109611. <https://doi.org/10.1016/j.foodhyd.2023.109611>
- Liu, C., Fan, L., Yang, Y., Jiang, Q., Xu, Y., & Xia, W. (2021). Characterization of surimi particles stabilized novel Pickering emulsions: Effect of particles concentration, pH and NaCl levels. *Food Hydrocolloids*, 117, Article 106731. <https://doi.org/10.1016/j.foodhyd.2021.106731>
- Liu, G., Wang, Q., Hu, Z., Cai, J., & Qin, X. (2019). Maillard-reacted whey protein isolates and epigallocatechin Gallate complex enhance the thermal stability of the Pickering emulsion delivery of curcumin. *Journal of Agricultural and Food Chemistry*, 67(18), 5212–5220. <https://doi.org/10.1021/acs.jafc.9b00950>
- Liu, L., Li, X., Du, L., Zhang, X., Yang, W., & Zhang, H. (2019). Effect of ultrasound assisted heating on structure and antioxidant activity of whey protein peptide grafted with galactose. *LWT - Food Science and Technology*, 109, 130–136. <https://doi.org/10.1016/j.lwt.2019.04.015>

- Lu, X., Zhang, H., Li, Y., & Huang, Q. (2018). Fabrication of milled cellulose particles-stabilized Pickering emulsions. *Food Hydrocolloids*, 77, 427–435. <https://doi.org/10.1016/j.foodhyd.2017.10.019>
- Ni, Z.-J., Liu, X., Xia, B., Hu, L.-T., Thakur, K., & Wei, Z.-J. (2021). Effects of sugars on the flavor and antioxidant properties of the Maillard reaction products of camellia seed meals. *Food Chemistry: X*, 11, Article 100127. <https://doi.org/10.1016/j.foodch.2021.100127>
- Nooshkam, M., Varidi, M., Zareie, Z., & Alkobeisi, F. (2023). Behavior of protein-polysaccharide conjugate-stabilized food emulsions under various destabilization conditions. *Food Chemistry: X*, 18, Article 100725. <https://doi.org/10.1016/j.foodch.2023.100725>
- Pan, Y., Wu, Z., Xie, Q.-T., Li, X.-M., Meng, R., Zhang, B., & Jin, Z.-Y. (2020). Insight into the stabilization mechanism of emulsions stabilized by Maillard conjugates: Protein hydrolysates-dextrin with different degree of polymerization. *Food Hydrocolloids*, 99, Article 105347. <https://doi.org/10.1016/j.foodhyd.2019.105347>
- Patel, A. R., & Dewettinck, K. (2015). Comparative evaluation of structured oil systems: Shellac oleogel, HPMC oleogel, and HIPE gel. *European Journal of Lipid Science and Technology*, 117(11), 1772–1781. <https://doi.org/10.1002/ejlt.201400553>
- Pirestani, S., Nasirpour, A., Keramat, J., Desobry, S., & Jasniewski, J. (2017). Effect of glycosylation with gum Arabic by Maillard reaction in a liquid system on the emulsifying properties of canola protein isolate. *Carbohydrate Polymers*, 157, 1620–1627. <https://doi.org/10.1016/j.carbpol.2016.11.044>
- Roy, S., Chawla, R., Santhosh, R., Thakur, R., Sarkar, P., & Zhang, W. (2023). Agar-based edible films and food packaging application: A comprehensive review. *Trends in Food Science & Technology*, 141, Article 104198. <https://doi.org/10.1016/j.tifs.2023.104198>
- Seo, C. W., & Oh, N. S. (2022). Functional application of Maillard conjugate derived from a κ-carrageenan/milk protein isolate mixture as a stabilizer in ice cream. *LWT - Food Science and Technology*, 161, Article 113406. <https://doi.org/10.1016/j.lwt.2022.113406>
- Seo, C. W., & Yoo, B. (2021). Preparation of milk protein isolate/κ-carrageenan conjugates by maillard reaction in wet-heating system and their application to stabilization of oil-in-water emulsions. *LWT - Food Science and Technology*, 139, Article 110542. <https://doi.org/10.1016/j.lwt.2020.110542>
- Song, X., Pei, Y., Qiao, M., Ma, F., Ren, H., & Zhao, Q. (2015). Preparation and characterization of Pickering emulsions stabilized by hydrophobic starch particles. *Food Hydrocolloids*, 45, 256–263. <https://doi.org/10.1016/j.foodhyd.2014.12.007>
- Su, J., Ma, Q., Cai, Y., Li, H., Yuan, F., Ren, F., ... Meeran, P. V. d. (2023). Incorporating surfactants within protein-polysaccharide hybrid particles for high internal phase emulsions (HIPEs): Toward plant-based mayonnaise. *Food Hydrocolloids*, 136, Article 108211. <https://doi.org/10.1016/j.foodhyd.2022.108211>
- Sun, L., Wang, D., Huang, Z., Elfalleh, W., Qin, L., & Yu, D. (2023). Structure and flavor characteristics of Maillard reaction products derived from soybean meal hydrolysates-reducing sugars. *LWT - Food Science and Technology*, 185, Article 115097. <https://doi.org/10.1016/j.lwt.2023.115097>
- Tang, X., Zhang, Y., Li, F., Zhang, N., Yin, X., Zhang, B., Zhang, B., Ni, W., Wang, M., & Fan, J. (2023). Effects of traditional and advanced drying techniques on the physicochemical properties of Lycium barbarum L. polysaccharides and the formation of Maillard reaction products in its dried berries. *Food Chemistry*, 409, Article 135268. <https://doi.org/10.1016/j.foodchem.2022.135268>
- Toker, O. S., Karasu, S., Yilmaz, M. T., & Karaman, S. (2015). Three interval thixotropy test (3ITT) in food applications: A novel technique to determine structural regeneration of mayonnaise under different shear conditions. *Food Research International*, 70, 125–133. <https://doi.org/10.1016/j.foodres.2015.02.002>
- Wang, L., Wu, M., & Liu, H.-M. (2017). Emulsifying and physicochemical properties of soy hull hemicelluloses-soy protein isolate conjugates. *Carbohydrate Polymers*, 163, 181–190. <https://doi.org/10.1016/j.carbpol.2017.01.069>
- Wang, W., Sheng, H., Zhou, J., Yuan, P., Zhang, X., Lu, M., & Gu, R. (2021). The effect of a variable initial pH on the structure and rheological properties of whey protein and monosaccharide gelation via the Maillard reaction. *International Dairy Journal*, 113, Article 104896. <https://doi.org/10.1016/j.idairyj.2020.104896>
- Wang, W.-D., Li, C., Chen, C., Fu, X., Hai, L., & Rui.. (2022). Effect of chitosan oligosaccharide glycosylation on the emulsifying property of lactoferrin. *International Journal of Biological Macromolecules*, 209, 93–106. <https://doi.org/10.1016/j.ijbiomac.2022.03.169>
- Wen, C., Zhang, J., Qin, W., Gu, J., Zhang, H., Duan, Y., & Ma, H. (2020). Structure and functional properties of soy protein isolate-lentinan conjugates obtained in Maillard reaction by slit divergent ultrasonic assisted wet heating and the stability of oil-in-water emulsions. *Food Chemistry*, 331, Article 127374. <https://doi.org/10.1016/j.foodchem.2020.127374>
- Wijaya, W., Meeran, P. V. d., Wijaya, C. H., & Patel, A. R. (2017). High internal phase emulsions stabilized solely by whey protein isolate-low methoxyl pectin complexes: Effect of pH and polymer concentration. *Food & Function*, 8(2), 584–594. <https://doi.org/10.1039/C6FO01027J>
- Xiao, J., Wang, X., Perez Gonzalez, A. J., & Huang, Q. (2016). Kafirin nanoparticles-stabilized Pickering emulsions: Microstructure and rheological behavior. *Food Hydrocolloids*, 54, 30–39. <https://doi.org/10.1016/j.foodhyd.2015.09.008>
- Xiao, Q., Chen, Z., Ma, M., Xie, X., Weng, H., Zhang, Y., Chen, J., & Xiao, A. (2023). Synthesis, characterization, antibacterial and emulsifying properties of agar benzoate. *International Journal of Biological Macromolecules*, 239, Article 124254. <https://doi.org/10.1016/j.ijbiomac.2023.124254>
- Xiao, Q., Chen, Z., Xie, X., Zhang, Y., Chen, J., Weng, H., Chen, F., & Xiao, A. (2022). A novel Pickering emulsion stabilized solely by hydrophobic agar microgels. *Carbohydrate Polymers*, 297, Article 120035. <https://doi.org/10.1016/j.carbpol.2022.120035>
- Xiao, Q., Ye, S., Zhang, Y., Chen, J., Chen, F., Weng, H., & Xiao, A. (2022). Gel properties transition from mono-succinylation to cross-linking of agar by attemperation with succinic anhydride. *Food Chemistry*, 381, Article 132164. <https://doi.org/10.1016/j.foodchem.2022.132164>
- Yalmanci, D., Dertli, E., Tekin-Cakmak, Z. H., & Karasu, S. (2023). Utilization of exopolysaccharide produced by Leuconostoc lactis GW-6 as an emulsifier for low-fat mayonnaise production. *International Journal of Biological Macromolecules*, 226, 772–779. <https://doi.org/10.1016/j.ijbiomac.2022.12.069>
- Ye, J., Hua, X., Zhao, Q., Dong, Z., Li, Z., Zhang, W., & Yang, R. (2020). Characteristics of alkali-extracted peanut polysaccharide-protein complexes and their ability as Pickering emulsifiers. *International Journal of Biological Macromolecules*, 162, 1178–1186. <https://doi.org/10.1016/j.ijbiomac.2020.06.245>
- Ye, S., Zhang, Y., Chen, J., Chen, F., Weng, H., Xiao, Q., & Xiao, A. (2022). Synthesis and properties of maleic anhydride-modified agar with reversibly controlled gel strength. *International Journal of Biological Macromolecules*, 201, 364–377. <https://doi.org/10.1016/j.ijbiomac.2021.12.096>
- Yu, K., Chen, W., Sheen, H., Chang, J., Lin, C., Ong, H., ... Ling, T. C. (2020). Production of microalgal biochar and reducing sugar using wet torrefaction with microwave-assisted heating and acid hydrolysis pretreatment. *Renewable Energy*, 156, 349–360. <https://doi.org/10.1016/j.renene.2020.04.064>
- Zhang, L., Xiao, Q., Zhang, Y., Weng, H., Wang, S., Chen, F., & Xiao, A. (2023). A comparative study on the gel transition, structural changes, and emulsifying properties of anhydride-esterified agar with varied degrees of substitution and carbon chain lengths. *Food Hydrocolloids*, 141, Article 108690. <https://doi.org/10.1016/j.foodhyd.2023.108690>
- Zhang, L., Ye, S., Chen, F., Xiao, Q., Weng, H., & Xiao, A. (2023). Super absorbent glutaric anhydride-modified agar: Structure, properties, and application in biomaterial delivery. *International Journal of Biological Macromolecules*, 231, Article 123524. <https://doi.org/10.1016/j.ijbiomac.2023.123524>
- Zhang, Y., Xu, J., Zhang, T., Tao, L., Nie, Y., Wang, X., & Zhong, J. (2022). Effect of carbon numbers and structures of monosaccharides on the glycosylation and emulsion stabilization ability of gelatin. *Food Chemistry*, 389, Article 133128. <https://doi.org/10.1016/j.foodchem.2022.133128>
- Zhang, Z., Chen, W., Zhou, X., Deng, Q., Dong, X., Yang, C., & Huang, F. (2021). Astaxanthin-loaded emulsion gels stabilized by Maillard reaction products of whey protein and flaxseed gum: Physicochemical characterization and in vitro digestibility. *Food Research International*, 144, Article 110321. <https://doi.org/10.1016/j.foodres.2021.110321>
- Zhang, Z., Wang, B., & Adhikari, B. (2022). Maillard reaction between pea protein isolate and maltodextrin via wet-heating route for emulsion stabilisation. *Future Foods*, 6, Article 100193. <https://doi.org/10.1016/j.fufo.2022.100193>
- Zhang, Z., Wang, X., Yu, J., Chen, S., Ge, H., & Jiang, L. (2017). Freeze-thaw stability of oil-in-water emulsions stabilized by soy protein isolate-dextran conjugates. *LWT - Food Science and Technology*, 78, 241–249. <https://doi.org/10.1016/j.lwt.2016.12.051>

Update

Carbohydrate Polymers

Volume 355, Issue , 1 May 2025, Page

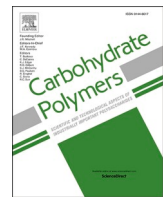
DOI: <https://doi.org/10.1016/j.carbpol.2025.123383>



Contents lists available at ScienceDirect

Carbohydrate Polymers

journal homepage: www.elsevier.com/locate/carbol



Corrigendum

Corrigendum to “Agar-gelatin Maillard conjugates used for Pickering emulsion stabilization” [Carbohydrate Polymers 340 (2024) 122293]



Lipeng Du, Yi Ru, Huifen Weng, Yonghui Zhang, Jun Chen, Anfeng Xiao, Qiong Xiao^{*}

College of Ocean Food and Biological Engineering, Jimei University, Xiamen 361021, PR China

National R&D Center for Red Alga Processing Technology, Xiamen 361021, PR China

Fujian Provincial Engineering Technology Research Center of Marine Functional Food, Xiamen 361021, PR China

Xiamen Key Laboratory of Marine Functional Food, Xiamen 361021, PR China

The authors sincerely apologize for an error that occurred during the process of merging the sub - figures of Fig. 5. Specifically, the sub - figures corresponding to pH 5 and pH 7 in Fig. 5E were mistakenly used repeatedly. At present, the image corresponding to pH 5 in Fig. 5E has

been corrected, while the corresponding textual content in the article remains unchanged.

Original version

DOI of original article: <https://doi.org/10.1016/j.carbol.2024.122293>.

* Corresponding author at: College of Ocean Food and Biological Engineering, Jimei University, Xiamen 361021, PR China.

E-mail address: xiaoqiong129@jmu.edu.cn (Q. Xiao).

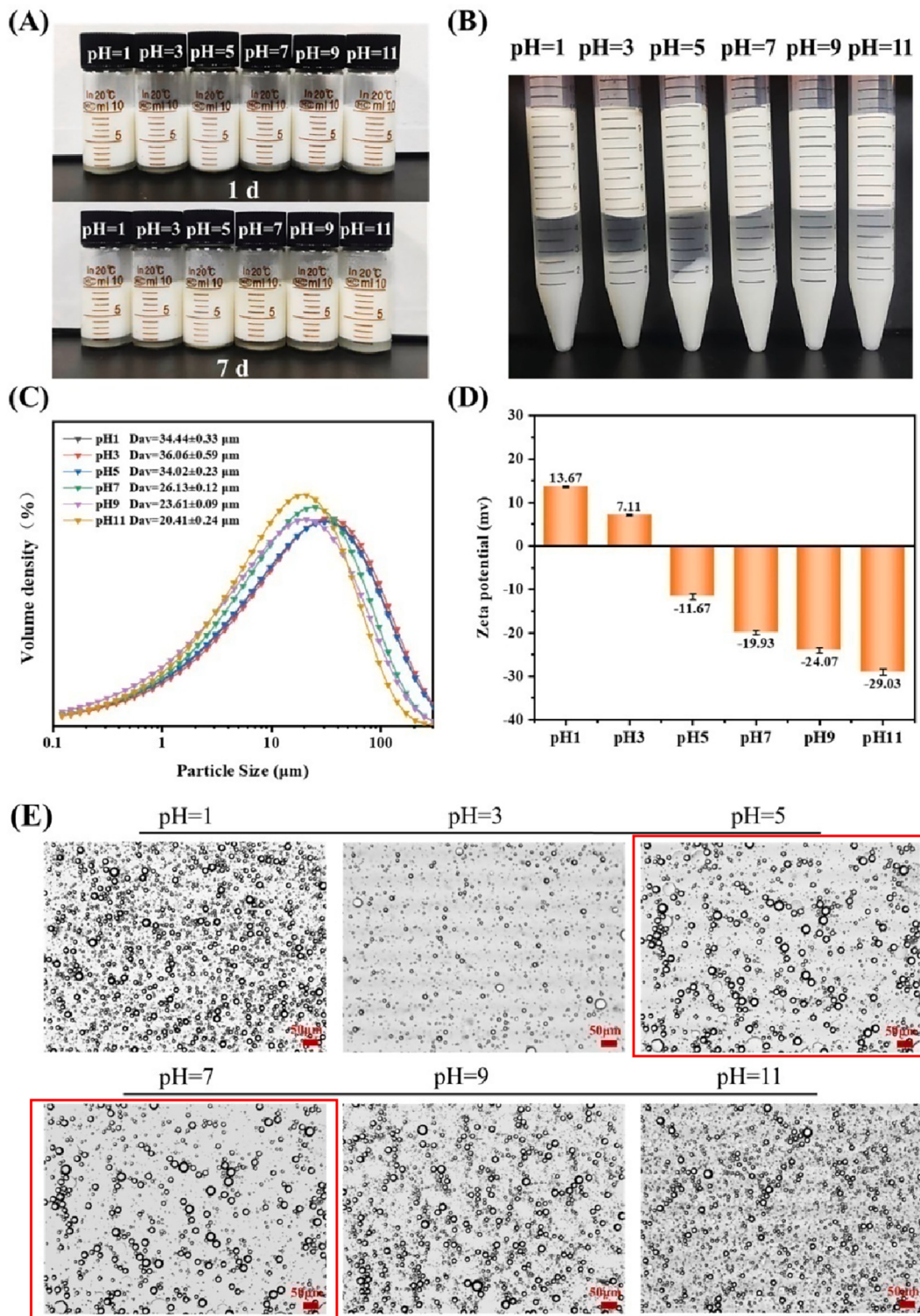


Fig. 5. Effect of pH on the stability of emulsions stabilized by agar-gelatin conjugates (AGMs). (A) appearance photograph of emulsions stored for 1 d and 7 d; (B) appearance photograph of emulsions after centrifugation at $3000 \times g$ for 20 min; (C) droplet size distribution of emulsions; (D) Zeta potential of emulsions at different pH conditions. (E) Optical micrographs ($100 \times$) of emulsion stored for 1 d, scale bar represent $50 \mu\text{m}$.

Revised version

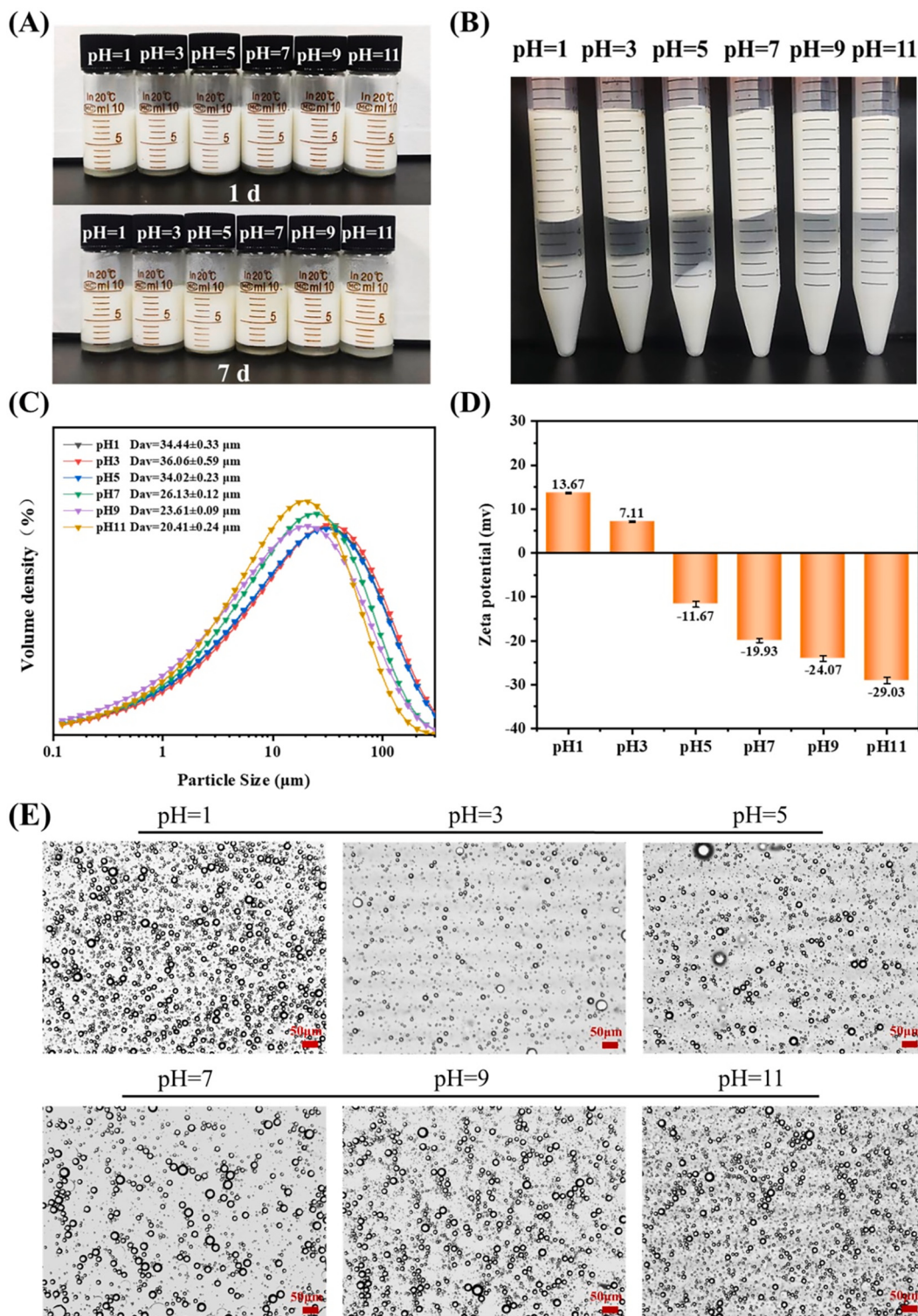


Fig. 5. Effect of pH on the stability of emulsions stabilized by agar-gelatin conjugates (AGMs). (A) appearance photograph of emulsions stored for 1 d and 7 d; (B) appearance photograph of emulsions after centrifugation at 3000 × g for 20 min; (C) droplet size distribution of emulsions; (D) Zeta potential of emulsions at different pH conditions. (E) Optical micrographs (100 ×) of emulsion stored for 1 d, scale bar represent 50 μm.

The authors would like to apologize for any inconvenience caused.